Inorg. Chem. **2002**, *41*, 5350–5363

Electronic Structure of Reduced Symmetry Peripheral Fused-Ring-Substituted Phthalocyanines

Nagao Kobayashi,*,† John Mack,‡ Kazuyuki Ishii,† and Martin J. Stillman*,‡

Department of Chemistry, Graduate School of Science, Tohoku University, Sendai 980-8578, Japan, and Department of Chemistry, University of Western Ontario, London, Ontario, Canada N6A 5B7

Received November 12, 2001

Reduced symmetry phthalocyanines are finding use in an increasing number of industrial applications. A detailed understanding of the electronic structure of the π-system will greatly facilitate the design of new complexes, which fit the specifications required in many of these emerging high technology fields. NMR, electronic absorption, magnetic circular dichroism (MCD), and fluorescence emission and excitation spectra have been recorded for five generic metal phthalocyanine (MPc) derivatives in which additional benzene rings are fused either radially or obliquely onto at least one of the four peripheral benzo groups. The spectroscopy of four radially substituted compounds, zinc mononaphthotribenzotetraazaporphyrine (Zn3B1N), zinc monobenzotrinaphthotetraazaporphyrine (Zn1B3N), and two cis and trans zinc dibenzodinaphthotetraazaporphyrine (Zn2B2N) isomers, is compared to that of the obliquely fused structural isomer of Zn3B1N (Zn3BoN) and the D_{4h} symmetry parent compounds, ZnPc and zinc naphthalocyanine (ZnNc). The selection of Zn(II) as the central metal eliminates the possibility of charge transfer between the metal and ring. None of the complexes studied contain any σ-bonded peripheral substituents. ^{1}H NMR signals of the seven compounds are assigned on the basis of the coupling patterns, integrated proton numbers, and decoupling experiments. The SIMPFIT program was used to perform spectral band deconvolution analyses of absorption and MCD spectra. ZINDO molecular orbital calculations are described, and the optical spectra are assigned on the basis of the MO models that have been developed previously to account for the spectral properties of metal porphyrin (MP(−2)) and metal phthalocyanine (MPc(−2)) complexes.

Introduction

Metal porphyrin complexes (MP(−2)) play a vital role in biological processes such as photosynthesis and respiration.[1] These complexes offer a unique chemistry that has several existing and potential industrial applications. The most commercially important group of the porphyrin class of molecules is the phthalocyanines, known systematically as tetrabenzo[5,10,15,20]tetraazaporphyrins.[2] Metal phthalocyanine complexes (MPc(−2)) have traditionally found use as dyes and pigments, and more recently as the photoconducting agent in photocopiers, because of their easy synthesis, high stability, and the presence of intense $\pi \rightarrow \pi^*$ transitions in the visible region.[3] In recent decades, there has been renewed interest in the use of phthalocyanine complexes in a variety of high technology fields including use in semi-

* To whom correspondence should be addressed. E-mail: Stillman@uwo.ca (M.J.S.); nagaok@mail.cc.tohoku.ac.jp (N.K.). Fax: (519) 661-3022. Phone: (519) 661-3821.

† Tohoku University, Sendai.

‡ University of Western Ontario.

(1) (a)*The Porphyrins*; Dolphin, D., Ed.; Academic Press: New York, 1978. (b) *Ann. N.Y. Acad. Sci.* **1973**, 206. (c) *The Porphyrin Handbook*; Kadish, K. M., Smith, K. M., Guilard, R., Eds.; Academic Press: New York, 1999.

(2) *Phthalocyanine. Properties and Applications*; Leznoff, C. C., Lever, A. B. P., Eds.; VCH Publications: New York, 1989; Vol. I. (b) *Phthalocyanine. Properties and Applications*; Leznoff, C. C., Lever, A. B. P., Eds.; VCH Publications: New York, 1993; Vol. II. (c) *Phthalocyanine. Properties and Applications*; Leznoff, C. C., Lever, A. B. P., Eds.; VCH Publications: New York, 1993; Vol. III. (d) *Phthalocyanine. Properties and Applications*; Leznoff, C. C., Lever, A. B. P., Eds.; VCH Publications: New York, 1996; Vol. IV.

(3) (a) Stillman, M. J.; Nyokong, T. In *Phthalocyanine. Properties and Applications*; Leznoff, C. C., Lever, A. B. P., Eds.; VCH Publications: New York, 1993; Vol. 1, Chapter 3, pp 133−290. (b) Stillman, M. J. In *Phthalocyanine. Properties and Applications*; Lever, A. B. P., Leznoff, C. C., Eds.; VCH Publications: New York, 1993; Part III, Chapter 5, pp 227−296. (c) Mack, J.; Stillman, M. J. *Coord. Chem Rev.* **2001**, *219*−*221*, 993. (d) Mack, J.; Stillman, M. J. *J. Porphyrins Phthalocyanines* **2001**, *5*, 67. (e) Mack, J.; Stillman, M. J. In *Handbook of Porphyrins and Related Macrocycles*; Kadish, K., Smith, K., Guilard, R., Eds.; Academic Press: New York, 2002. (f) VanCott, T. C.; Rose, J. L.; Misener, G. C.; Williamson, B. E.; Schrimpf, A. E.; Boyle. M. E.; Schatz, P. N. *J. Phys. Chem.* **1989**, *93*, 2999.

10.1021/ic011152d CCC: $22.00
Published on Web 09/27/2002

conductor devices,[4] photovoltaic and solar cells,[5] electrophotography,[6] rectifying devices,[7] molecular electronics,[8] Langmuir−Blodgett films,[9] electrochromism in display devices,[10] low dimensional metals,[11] gas sensors,[12] liquid crystals,[13] and nonlinear optics,[14] and as photosensitizers[15] and electrocatalytic agents.[16] In a number of these applications, the wavelength of the major $\pi \rightarrow \pi^*$ transitions in the UV−vis region is of critical importance. Because it is impossible to find an MPc(−2) complex that absorbs significantly for all desired wavelengths, there is considerable current interest in the electronic spectroscopy of structurally modified MPc(−2) molecules.[17−22] A detailed understanding of the impact of different structural modifications on the electronic structure will greatly assist the development of new industrial applications for these molecules because it will facilitate the selection of previously uncharacterized molecules with a set of desired spectral properties via computer modeling.

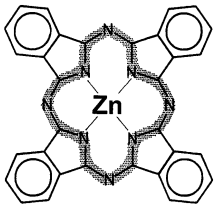

Figure 1. Molecular structure of a typical main group metal phthalocyanine showing the path of the 16-atom cyclic polyene ring that forms the basis of the 4-orbital calculations of Gouterman used to account for the two lowest energy major $\pi \rightarrow \pi^*$ transitions of porphyrins and phthalocyanines.

In its simplest description, the optical spectroscopy of the π-system of MP(−2) and MPc(−2) can be accounted for by considering only the 16-atom, 18-π-electron cyclic polyene aromatic ring that runs around the inner perimeter of the ligand, Figure 1. Gouterman's model, based on a 4-orbital linear combination of atomic orbitals (LCAO), has been widely used to describe the optical spectra of both MP(−2) and MPc(−2) complexes.[3,23−26] In an ideal 16-atom, 18-π-electron cyclic polyene, the HOMO has an M_L value of ± 4 while the LUMO has an M_L value of ± 5. This scheme predicts an allowed B transition ($\Delta M_L = \pm 1$) and a forbidden Q transition ($\Delta M_L = \pm 9$). MCD spectroscopy has confirmed the allowed and forbidden nature of the Q and B bands of MP(−2).[27] The A_1/D_0 ratio (the MCD A term intensity divided by the absorption intensity) provides a direct spectral measurement of the angular momentum of the excited state. Gouterman's group demonstrated the validity of the 4-orbital approach through more detailed molecular orbital calculations.[25,28] Although Gouterman's models were developed over 30 years ago, no subsequent theoretical calculations have been reported that account for the optical spectra of MP(−2) and MPc(−2) complexes in a more satisfactory manner.[29] Gouterman's model has, therefore, been used as

(4) Simon, J.; Andre, J.-J. In *Molecular Semiconductors*; Springer: Berlin, 1985; Chapter 3.
(5) (a) Wöhrle, D.; Meissner, D. *Adv. Mater.* **1991**, *3*, 129. (b) Tang, C. W. *Appl. Phys. Lett.* **1986**, *60*, 1047.
(6) Loutfy, R. O.; Hor, A. M.; Hsiao, C. K.; Baranyi, G.; Kazmaier, P. *Pure Appl. Chem.* **1988**, *60*, 1047.
(7) Abe, K.; Sato, H.; Kimura, T.; Ohkatsu, Y.; Kusano, T. *Makromol. Chem.* **1989**, *190*, 2693.
(8) Simic-Glavaski, B. In *Phthalocyanine. Properties and Applications*; Leznoff, C. C., Lever, A. B. P., Eds.; VCH Publications: New York, 1993; Vol. III, Chapter 3, pp 119−166.
(9) (a) Roberts, G. G.; Petty, M. C.; Baker, S.; Fowler, M. T.; Thomas, N. J. *Thin Solid Films* **1985**, *132*, 113. (b) Cook, M. J.; Dunn, A. J.; Daniel, M. F.; Hart, R. C. O.; Richardson, R. M.; Roser, S. J. *J. Am. Chem. Soc.* **1988**, *159*, 395. (c) Palacin, S.; Lesieur, P.; Stefanelli, I.; Barraud, A. *J. Am. Chem. Soc.* **1988**, *110*, 83.
(10) Nicholson, M. M. In *Phthalocyanine. Properties and Applications*; Leznoff, C. C., Lever, A. B. P., Eds.; VCH Publications: New York, 1993; Vol. III, Chapter 2, pp 71−118.
(11) (a) Marks, T. J. *Angew. Chem., Int. Ed. Engl.* **1990**, *29*, 857. (b) Hanack, M.; Datz, A.; Fay, R.; Fischer, K.; Keppeler, U.; Koch, J.; Metz, J.; Mezger, M.; Schneider, O.; Schulze, H. J. In *Handbook of Conducting Polymers*; Skotheim, T. A. B., Ed.; Marcel Dekker: New York, 1986; Vol. 1, Chapter 5, p 133.
(12) Snow, A. W.; Barger, W. R. In *Phthalocyanine. Properties and Applications*; Leznoff, C. C., Lever, A. B. P., Eds.; VCH Publications: New York, 1989; Vol. I, Chapter 3, pp 341−392.
(13) (a) Van der Pol, J. F.; Neeleman, E.; Zwikker, J. W.; Nolte, R. J. M.; Drenth, W.; Aerts, J.; Visser, R.; Picken, S. J. *Liq. Cryst.* **1989**, *6*, 577. (b) Simon, J.; Sirlin, C. *Pure Appl. Chem.* **1989**, *61*, 1625.
(14) (a) Casstevens, M. K.; Samoc, M.; Pfleger, J.; Prasad, P. M. *J. Chem. Phys.* **1990**, *92*, 2019. (b) Simon, J.; Bassoul, P.; Norvez, S. *New J. Chem.* **1989**, *13*, 13. (c) *Nonlinear Optics of Organic Molecules and Polymers*; Nalwa, H. S., Miyata, S., Eds.; CRC Press: Boca Raton, FL, 1997. (d) de la Torre, G.; Vazuez, P.; Agullo-Lopez, F.; Torres, T. *Adv. Mater.* **1997**, *9*, 265.
(15) Kato, M.; Nishioka, Y.; Kaifu, K.; Kawamura, K.; Ohno, S. *Appl. Phys. Lett.* **1985**, *46*, 196.
(16) Lever, A. B. P.; Hempstead, M. R.; Leznoff, C. C.; Lin, W.; Melnik, M.; Nevin, W. A.; Seymour, P. *Pure Appl. Chem.* **1986**, *18*, 1467.
(17) (a) Leznoff, C. C.; Hall, T. W. *Tetrahedron Lett.* **1982**, *23*, 3023. (b) Hall, T. W.; Greenberg, S.; McArther, C. R.; Khouw, B.; Leznoff, C. C. *Nouv. J. Chim.* **1982**, *6*, 653. (c) Tse, Y. H.; Goel, A.; Hu, M.; Lever, A. B. P.; Leznoff, C. C.; Van Lier, J. E. *Can. J. Chem.* **1993**, *71*, 742. (d) Fu, Y.; Forman, M.; Leznoff, C. C.; Lever, A. B. P. *J. Phys. Chem.* **1994**, *98*, 8985. (e) McKeown, N. B.; Leznoff, C. C. *Mol. Cryst. Liq. Cryst.* **1992**, *213*, 91. (f) Nolan, K. J. M.; Hu, M.; Leznoff, C. C. *Synlett* **1997**, 593.
(18) (a) Ikeda, Y.; Konami, H.; Hatano, M.; Mochizuki, K. *Chem. Lett.* **1992**, 763. (b) Kobayashi, N.; Ashida, T.; Osa, T. *Chem. Lett.* **1992**, 2031. (c) Konami, H.; Ikeda, Y.; Hatano, M.; Mochizuki, K. *Mol. Phys.* **1993**, *80*, 153. (e) Kobayashi, N.; Ashida, T.; Osa, T.; Konami, H. *Inorg. Chem.* **1994**, *33*, 1735. (f) Kobayashi, N. *Chem. Commun.* **1998**, 487. (g) Miwa, H.; Kobayashi, N. *Chem. Lett.* **1999**, 1303.
(19) (a) Kobayashi, N. In *Phthalocyanine. Properties and Applications*; Leznoff, C. C., Lever, A. B. P., Eds.; VCH Publications: New York, 1989; Vol. 2, Chapter 3, pp 97−163. (b) Kobayashi, N.; Konami, H. In *Phthalocyanine. Properties and Applications*; Leznoff, C. C., Lever, A. B. P., Eds.; VCH Publications: New York, 1996; Vol. 4, Chapter 9, pp 343−404.
(20) (a) Cook, M. J.; Jafari-Fini, A. *J. Mater. Chem.* **1997**, *7*, 5. (b) Cook, M. J.; Jafari-Fini, A. *J. Mater. Chem.* **1997**, *7*, 2327. (c) McKeown, N. B.; Chambrier, I.; Cook, M. J. *J. Chem. Soc., Perkin Trans I* **1990**, 1169.
(21) Bauman, T. F.; Sibert, J. W.; Olmstead, M. M.; Barrett, A. G. M.; Hoffman, B. M. *J. Am. Chem. Soc.* **1994**, *116*, 2639. Bauman, T. F.; Nasir, M. S.; Sibert, J. W.; White, A. J. P.; Olmstead, M. M.; Williams, D. J.; Barrett, A. G. M.; Hoffman, B. M. *J. Am. Chem. Soc.* **1996**, *118*, 10479.
(22) (a) Nicolau, M.; Cabezon, B.; Torres, T. *Coord. Chem. Rev.* **1999**, *190−192*, 231−243. (b) Sastre, A.; del Ray, B.; Torres, T. *J. Org. Chem.* **1996**, *61*, 8591. (c) Cabezon, B.; Rodriguez-Morgade, T. *J. Org. Chem.* **1995**, *60*, 1872. (d) de la Torre, G.; Torres, T. *J. Org. Chem.* **1996**, *61*, 6446.
(23) (a) Gouterman, M. In *The Porphyrins*; Dolphin, D., Ed.; Academic Press: New York, 1978; Vol. III, Part A, pp 1−165. (b) Gouterman, M. *J. Mol. Spectrosc.* **1972**, *44*, 37. (c) Gouterman, M.; Wagniere, G. H.; Snyder, L. C. *J. Mol. Spectrosc.* **1963**, *11*, 108.
(24) (a) Michl, J. *J. Am. Chem. Soc.* **1978**, *100*, 6801. (b) Michl, J. *Pure Appl. Chem.* **1980**, *52*, 1549.
(25) Weiss, C.; Kobayashi, H.; Gouterman, M. *J. Mol. Spectrosc.* **1965**, *16*, 415.
(26) McHugh, A. J.; Gouterman, M.; Weiss, C. *Theor. Chim. Acta* **1972**, *24*, 346.
(27) Briat, B.; Schooley, D. A.; Records, R.; Bunnenberg, E.; Djerassi, C. *J. Am. Chem. Soc.* **1967**, *89*, 7062.
(28) Schaffer, A. M.; Gouterman, M.; Davidson, E. R. *Theor. Chim. Acta* **1973**, *30*, 9.

the theoretical framework within which to assign the bands observed in the optical spectra of a variety of MP(−2) and MPc(−2) complexes and their cation and anion radical species on the basis of spectral deconvolution studies of the UV−vis absorption and magnetic circular dichroism (MCD) spectroscopy[3c,e,30] using the SIMPFIT program.[3a,e,31−36] The major $\pi \rightarrow \pi^*$ bands within the UV−vis region of MPc(−2) optical spectra are currently referred to as Q, B1, B2, N, L, and C in a sequence ordered by ascending energy on the basis of Gouterman's nomenclature.

The spectroscopy of structurally modified phthalocyanine complexes has received considerably less attention than that of MPc(−2) complexes with D_{4h} symmetry.[3] The impact of reducing the molecular symmetry through asymmetric σ-bonded substitution of the peripheral protons has been explored. The spectral changes observed are primarily related to the electron withdrawing or donating effects of the substituents on the π-system and are usually confined to slight shifts in the wavelengths of the major band centers.[3,37] In a recent paper, we studied the spectral changes that result from partial aza-nitrogen substitution at the 5, 10, 15, and 20 bridging positions of tetrabenzoporphyrin.[38] In this paper, we study the spectral impact of extending the π-system through asymmetric peripheral, fused benzene-ring substitutions. The extension of the π-system through peripheral aliphatic groups in naturally occurring porphyrin molecules such as protoporphyrin IX normally has only a minor impact on the optical spectroscopy. High molecular symmetry would still be inferred for these compounds on the basis of the MCD spectra because the peripheral substituents exert only a marginal influence on the spectroscopy of the inner perimeter cyclic polyene aromatic π-system.[39] Recent studies on the impact of ring expansion in the case of symmetric subazaporphyrin, subphthalocyanine, and subnaphthalocyanine complexes have indicated that extending the π-system has a much more profound impact on the spectroscopy of the π-system.[40] Expansion of the heteroaromatic π-system by adding additional fused benzene rings offers the potential of maintaining the planarity of the π-system and a well-defined molecular symmetry while unambiguously modifying both the spectroscopic properties and electronic structure. Because many of the most industrially useful properties of MPc complexes are related directly to the planar heteroaromatic nature of the π-system, this structural modification should introduce new properties with considerable potential for use in new industrial applications.

The molecular structures of the five asymmetric peripheral fused ring expanded complexes studied in this paper are shown in Figure 2. Zinc mononaphthotribenzotetraazaporphyrine (Zn3B1N) and monobenzotrinaphthotetraazaporphyrine (Zn1B3N) have C_{2v}(III) symmetry, while the cis and trans isomers of dibenzodinaphthotetraazaporphyrine (Zn2B2N) have C_{2v}(III) and D_{2h} symmetry, respectively. In C_{2v}(III) symmetry, the C_2 axis does not correspond to the main 4-fold axis of symmetry of MPc(−2) but lies instead within the plane of the π-system.[41] Zn3BoN is a lower symmetry structural isomer of Zn3B1N in which the additional outer fused ring is rotated obliquely out of alignment with the axes of symmetry of ZnPc resulting in C_s symmetry. NMR, electronic absorption, magnetic circular dichroism (MCD), and fluorescence emission and excitation spectroscopies are used to explore the impact of these structural modifications to the π-system. Because the complexes studied do not contain any peripheral substituent groups, ^{1}H NMR can be used to study the ring current generated by these five reduced symmetry heteroaromatic ligands. Zinc was selected as the central metal to eliminate ligand to metal and metal to ligand charge transfer bands. These spectra should, therefore, form a generic template for understanding the spectroscopy of this entire class of reduced symmetry phthalocyanine complexes.

Experimental Section

(a) Synthesis. ZnPc(−2), Zn3B1N, Zncis2B2N, Zntrans2B2N, Zn1B3N, and ZnNc(−2) were synthesized by the mixed condensation method.[18a] Octabutoxylated complexes analogous to Zn3B1N, Zncis2B2N, Zntrans2B2N, and Zn1B3N have been reported previously.[42] Zn3BoN was obtained by mixing 1,2-dicyanonaphthalene (1 equiv), zinc acetate (1.1 equiv), hydroquinone (1 equiv), and phthalonitrile (3 equiv) and heating at 270 °C under nitrogen for 5 min. The residue was washed with water and methanol at room temperature and dissolved in THF for alumina column chromatography. The blue-green portion was isolated by gel-permeation chromatography using Bio-beads SX-8 (Bio-rad) and THF as eluent. Because the blue-green bands were not fully resolved, fractions were collected in a number of sample tubes and their electronic absorption spectra compared. By repeating this procedure several times, portions that gave a similar absorption spectrum were

(29) (a) Henriksson, A.; Roos, B.; Sundbom, M. *Theor. Chim. Acta* **1972**, *27*, 303. (b) Dedieu, A.; Rohmer, M.-M.; Veillard, A. *Adv. Quantum Chem.* **1982**, *16*, 43. (c) Orti, E.; Bredas, J. L.; Clarisse, C. *J. Chem. Phys.* **1990**, *92*, 1228. (d) Liang, X. L.; Flores, S.; Ellis, D. E.; Hoffman, B. M.; Musselman, R. L. *J. Chem. Phys.* **1991**, *95*, 403. (e) Rosa, A.; Baerends, E. J. *Inorg. Chem.* **1992**, *31*, 4717. (f) Rosa, A.; Baerends, E. J. *Inorg. Chem.* **1994**, *33*, 584. (g) Ishikawa, N.; Ohno, O.; Kaizu, Y.; Kobayashi, H. *J. Phys. Chem.* **1992**, *96*, 8832. (h) Ishikawa, N.; Ohno, O.; Kaizu, Y. *J. Phys. Chem.* **1993**, *97*, 1004. (i) Liao, M.-S.; Scheiner, S. *J. Chem. Phys.* **2001**, *114*, 9780. (j) Ricciardi, G.; Rosa, A.; Barends, E. J. *J. Phys. Chem. A* **2001**, *105*, 5242. (k) Nguyen, K. A.; Pachter, R. *J. Chem. Phys.* **2001**, *114*, 10757.

(30) (a) Piepho, S. B.; Schatz, P. N. In *Group Theory in Spectroscopy with Applications to Magnetic Circular Dichroism*; Wiley: New York, 1983. (b) Stephens, P. J. *Adv. Chem. Phys.* **1976**, *35*, 197.

(31) (a) Nyokong, T.; Gasyna, Z.; Stillman, M. J. *Inorg. Chem.* **1987**, *26*, 548. (b) Nyokong, T.; Gasyna, Z.; Stillman, M. J. *Inorg. Chem.* **1987**, *26*, 1087.

(32) Ough, E. A.; Nyokong, T.; Creber, K. A. M.; Stillman, M. J. *Inorg. Chem.* **1988**, *27*, 2724.

(33) Ough, E. A.; Gasyna, Z.; Stillman, M. J. *Inorg. Chem.* **1991**, *30*, 2301.

(34) Gasyna, Z.; Stillman, M. J. *Inorg. Chem.* **1990**, *29*, 5101.

(35) Mack, J.; Stillman, M. J. *J. Am. Chem. Soc.* **1994**, *116*, 1292.

(36) Mack, J.; Stillman, M. J. *J. Phys. Chem.* **1995**, *99*, 7935.

(37) Golovin, M. N.; Seymour, P.; Jayaraj, K.; Fu, Y.; Lever, A. B. P. *Inorg. Chem.* **1990**, *29*, 1719.

(38) Mack, J.; Kobayashi, N.; Leznoff, C. C.; Stillman, M. J. *Inorg. Chem.* **1997**, *36*, 5624.

(39) (a) Nozawa, T.; Ookubo, S.; Hatano, M. *J. Inorg. Biochem.* **1980**, *12*, 253. (b) Pond, A. E.; Roach, M. P.; Sono, M.; Rux, A. H.; Franzen, S.; Hu, R.; Thomas, M. R.; Wilks, A.; Dou, Yi; Ikedo-Saito, M.; Ortiz de Montellano, P. R.; Woodruff, W. H.; Dawson, J. H. *Biochemistry* **1999**, *38*, 7601.

(40) Kobayashi, N.; Ishizaki, T.; Ishii, K.; Konami, H. *J. Am. Chem. Soc.* **1999**, *121*, 9096.

(41) Donini, J. C.; Hollebone, B. R.; Lever, A. B. P. *Prog. Inorg. Chem.* **1977**, *22*, 225.

(42) Aoudia, M.; Cheng, G.; Kennedy, V. O.; Kenney, M. E.; Rodgers, A. J. *J. Am. Chem. Soc.* **1997**, *119*, 6029.

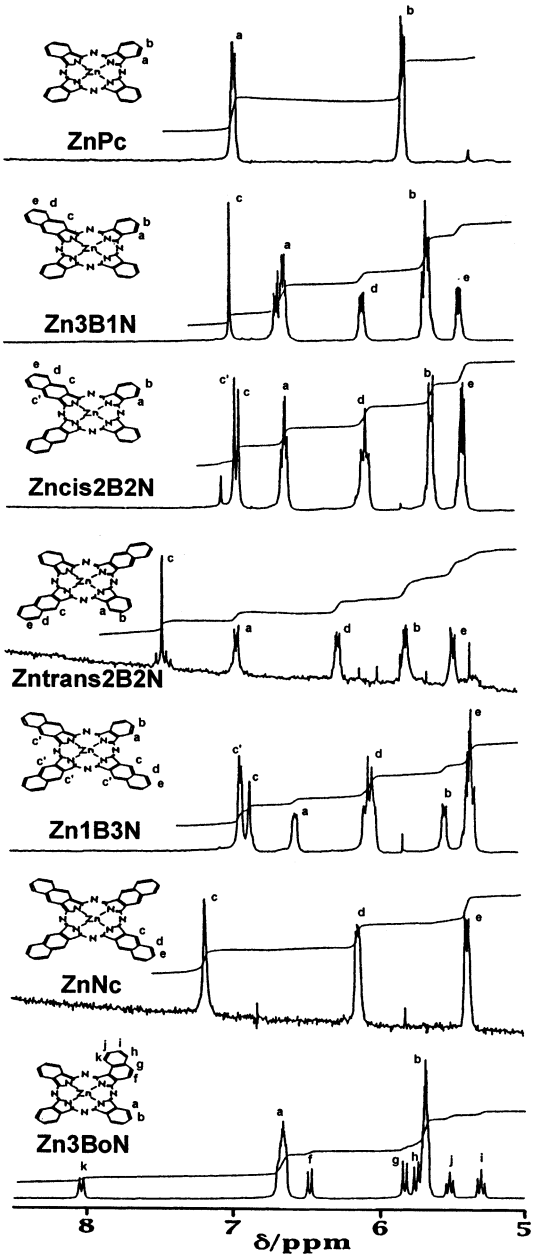

Figure 2. ^{1}H NMR spectra and molecular structures of ZnPc(−2) **1**, Zn3B1N **2**, Zncis2B2N **3**, Zntrans2B2N **4**, Zn1B3N **5**, ZnNc(−2) **6**, and Zn3BoN **7**.

collected, concentrated, and recrystallized twice from THF. Analysis yielded C, 69.05; H, 3.11; N, 17.52, which is in good agreement with the anticipated C, 68.85; H, 2.89; N, 17.84. The parent *m*/*z* peak of 626 was observed by FAB mass spectrometry using a *m*-nitrobenzyl alcohol matrix.

(b) Optical Spectroscopy. UV−vis spectra were recorded with a Shimadzu UV-250 spectrophotometer, and magnetic circular dichroism (MCD) measurements were made with a JASCO J-720 spectrodichrometer. The JASCO electromagnet has a maximum field strength of 1.09 tesla (T). MCD intensity is expressed in terms of molar ellipticity per tesla, $[\theta]_M = 10^4$ deg mol^{-1} dm^3 cm^{-1} T^{-1}, and $\Delta\epsilon_M$, where $[\theta]_M = 3300\Delta\epsilon_M$. Fluorescence and excitation spectra were recorded with a Shimadzu RF-500 spectrofluorimeter with appropriate filters to eliminate scattered light. Fluorescence quantum yields (Φ_F) were determined by the comparative calibration method through the use of H_2Pc ($\Phi_F = 0.60$) and ZnPc ($\Phi_F = 0.30$)[43] or 1,3,3,1′,3′,3′-hexamethylindotricarbocyanine ($\Phi_F = 0.28$)[44] as standards. All solutions were purged with argon prior to fluorescence spectral measurement.

(c) NMR Spectroscopy. ^{1}H NMR spectra were recorded with a JEOL GX-500 500 MHz spectrometer in dimethyl sulfoxide-d_6 with tetramethylsilane (TMS) as the standard. Because of the low solubility of many of the complexes studied (particularly Zntrans-2B2N and ZnNc(−2)) due to the absence of peripheral substituents, the signal had to be accumulated by averaging between 6000 and 48000 scans. The ^{1}H signals obtained were assigned on the basis of the integrated intensities, coupling patterns, and the results of decoupling experiments, Figure 2.

(d) MCD Spectroscopy. MCD spectroscopy provides the ground and excited state degeneracy information, which is required to fully understand the electronic structure of high symmetry molecules. The additional information provided by the MCD technique is derived from three highly characteristic spectral features, the Faraday A, B, and C terms.[30] The derivative-shaped Faraday A term is temperature independent and identifies degenerate excited states, while the normally Gaussian-shaped C term is highly temperature dependent and identifies an orbitally degenerate ground state. Gaussian-shaped, temperature independent B terms arise from field-induced mixing between closely related states linked by a magnetic dipole transition moment. The ground states of divalent, main group D_{4h} MPc(−2) complexes are nondegenerate ($^1A_{1g}$), and the accessible $\pi \rightarrow \pi^*$ excited states are orbitally degenerate (^1E_u). The MCD spectra are therefore dominated by intense *x*/*y*-polarized derivative-shaped A terms, Figure 3. Vibronically coupled and n $\rightarrow \pi^*$ states can also transform as $^1A_{2u}$, giving rise to *z*-polarized B terms. Complexes with symmetry lower than D_{4h} give rise to oppositely signed coupled B terms usually with *x*- and *y*-polarization rather than A terms in the MCD spectra. The ordering of the sign of the A terms to high energy is not related to the polarization of the bands but to the orbital angular momentum associated with the ground and excited states in the absence of the perturbation to the D_{4h} symmetry of the inner cyclic polyene.[24] The ground state of Zntrans2B2N is ^1A_g, and the accessible $\pi \rightarrow \pi^*$ excited states are $^1B_{3u}$ and $^1B_{2u}$ under D_{2h} symmetry. In the case of Zn3B1N, Zncis2B2N, and Zn1B3N, the ground state is $^1A_1$, and the accessible $\pi \rightarrow \pi^*$ excited states are $^1A_1$ and $^1B_1$ under C_{2v}(III) symmetry giving rise to B terms of *x*- and *z*-polarization. The ground and excited states of the C_s symmetry Zn3BoN complex are $^1A'$.

(e) Band Fitting using SIMPFIT. Band deconvolution has the potential to provide quantitative parameters for the allowed electronic transitions in extensively overlapped spectral envelopes. The major problem associated with band deconvolution analyses is that many different potential fits can usually be made for a single spectral data set. The unique approach developed during the design of the SIMPFIT program[3e,45,46] overcomes this problem through the simultaneous spectral deconvolution of the MCD and absorption spectral data sets recorded on the same solution. The MCD signal arises from the same electronic transitions as the UV−vis absorption spectrum, but the selection rules are different because the intensity mechanism depends on the magnetic dipole moment in addition to the electric dipole moment. The approach used in the SIMPFIT program rests on the fact that under the rigid shift assumption it can be assumed that the application of a magnetic field will make no difference to the spectral band shape function.[30] Fitting two

(43) Seybold, P. G.; Gouterman, M. *J. Mol. Spectrsc.* **1969**, *31*, 1.
(44) Duggan, J. X.; Lesare, J. D.; Williams, J. F. *ASTM Spec. Tech. Publ.* **1983**, 822.
(45) Mack, J.; Browett, W.; Stillman, M. J. To be submitted for publication.
(46) Gasyna, Z.; Browett, W. R.; Nyokong, T.; Kitchenham, R.; Stillman, M. J. *Chemom. Intell. Lab. Syst.* **1989**, *5*, 233.

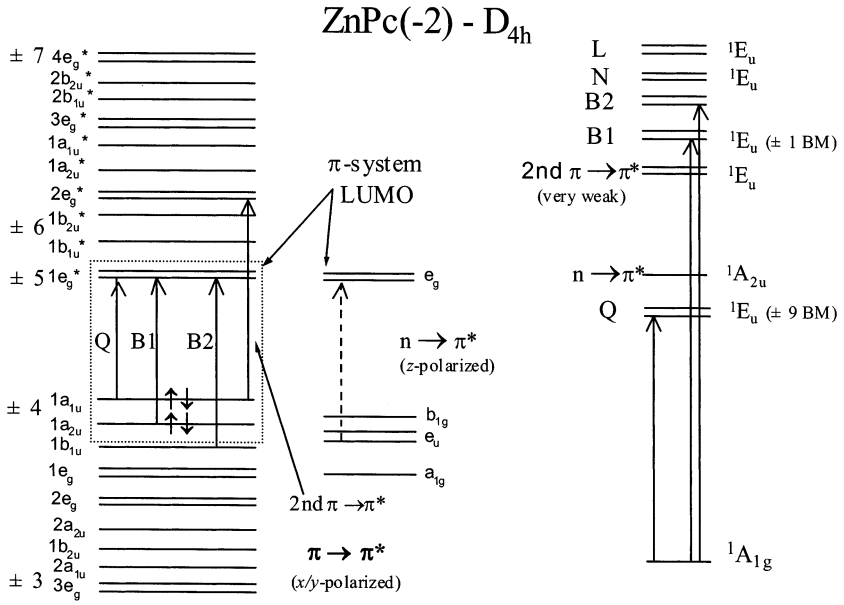

Figure 3. Molecular orbital (A) and state level (B) diagrams of MPc(−2) showing the one-electron transitions that are predicted to give rise to absorption bands in the 280−1000 nm range. The orbital ordering on the left is based on Gouterman's model of the inner ring cyclic polyene.[23] The orbitals on the right are the four aza-nitrogen lone pair orbitals. The Q, second $\pi \rightarrow \pi^*$, B1, B2, N, and L bands have been identified through spectral deconvolution studies[3a,e,31−36] on the basis of Gouterman's SCMO-PPP-CI model.[28] The ordering of the MOs is based on more recent ZINDO calculations.[54] Transitions that give rise to *x*/*y*-polarized bands are represented with solid lines. Dashed lines are used for *z*-polarized transitions. The nπ^* excited state is placed between the Q and B1 $\pi\pi^*$ excited states on the basis of a spectral deconvolution analysis of (CN^-)ZnPc(−2).[36]

spectra recorded on the same solution with different band morphologies on the basis of two separate sets of selection rules with the same basic parameters removes much of the ambiguity that is normally associated with band deconvolution analyses. A new updated version of SIMPFIT[45] developed using Visual Basic was used during the band fitting reported in this paper.

(f) ZINDO Molecular Orbital Calculations. The structures for the ZINDO calculations, Figure 2, were developed through the use of a Fujitsu Inc. CAChe workstation.[47] The structures were then refined using a modified MM2 force field calculation in the Mechanics program of the CAChe system.[48] The structures were optimized at the restricted Hartree−Fock self-consistent field (SCF) level[49] using the ZINDO program in the CAChe software package.[50,51] These SCF optimizations were carried out at the intermediate neglect of differential overlap/1[52] (INDO/1) level of approximation. The structures were then used to calculate the UV−vis absorption spectra shown in Tables 1−3 and Tables S1−S3 (Supplementary Information). The active orbitals in the ZINDO/s configuration interaction (CI) calculation were the 25 lowest energy unoccupied and 25 highest energy occupied MOs. The heteroaromatic π-systems of the five complexes studied, Figure 2, have a well-defined planar structure. The results obtained from ZINDO geometry optimization are therefore expected to be very similar to those obtained from other commonly used techniques such as density functional theory (DFT).[53] This was confirmed by running DFT geometry optimizations in which the B88-PW91 GGA function was used with DZVP basis sets.

Results and Discussion

ZINDO Calculations. The calculated energies of the π-system MOs of a D_{4h} 16 atom 18 π−electron cyclic polyene $ZnC_8N_8H_{16}$ model complex (ZnCP), zinc tetraazaporphyrin (ZnTAP), ZnPc, Zn3B1N, Zn3BoN, Zncis2B2N, Zntrans2B2N, Zn1B3N, and ZnNc(−2) in the −11 to 3 eV range are shown schematically in Table 4 and Figure 4. The distinctive nodal and antinodal patterns observed for ZnPc(−2) MOs are observed consistently over the entire series of complexes. The orbitals have, therefore, been ordered relative to the corresponding ZnPc(−2) orbital so that the one-electron transitions responsible for the bands in the ZINDO calculated spectra of each complex can be directly compared to the existing model developed for the high symmetry parent complex.[54] The energies of σ-MOs associated primarily with the aza- and pyrrole-nitrogen lone pair orbitals in the −11 to 3 eV range are shown in Table 5. The correlation of the b_{1u}, b_{2u}, b_{1g}, and b_{2g} orbitals is different in the case of Zncis2B2N from that of Zn3B1N and Zn1B3N because the 2-fold axis of symmetry corresponds to the c_2' and not the c_2'' axes of ZnPc(−2) and the symmetry of these orbitals is primarily dependent on the symmetry operations associated with these axes.

(47) CAChe Scientific P.O. Box 500, Mail Station 13-400 Beaverton, OR 97077.
(48) Purvis, G. D., III. *Comput. Aided Mol. Des.* **1991**, *5*, 55.
(49) Roothaan, C. C. J. *Rev. Mod. Phys.* **1951**, *23*, 69.
(50) (a) Ridley, J. E.; Zerner, M. C. *Theor. Chim. Acta* **1973**, *32*, 111. (b) Zerner, M. C.; Loew, G. H.; Kirchner, R. F.; Mueller-Westerhoff, U. T. *J. Am. Chem. Soc.* **1980**, *102*, 589. (c) Ridley, J. E.; Zerner, M. C. *Theor. Chim. Acta* **1976**, *42*, 223. (d) Bacon, A.; Zerner, M. C. *Theor. Chim. Acta* **1979**, *53*, 21.
(51) (a) Head, J.; Zerner, M. C. *Chem. Phys. Lett.* **1985**, *122*, 264. (b) Head, J.; Zerner, M. C. *Chem. Phys. Lett.* **1986**, *131*, 359. (c) Anderson, W.; Edwards, W. D.; Zerner, M. C. *Inorg. Chem.* **1986**, *25*, 2728. (d) Edwards, W. D.; Zerner, M. C. *Theor. Chim. Acta* **1987**, *72*, 347. (e) Kotzian, M.; Roesch, N.; Zerner, M. C. *Theor. Chim. Acta* **1992**, *81*, 201. (f) Kotzian, M.; Roesch, N.; Zerner, M. C. *Int. J. Quantum Chem.* **1991**, 545.
(52) Pople, J. A.; Beveridge, D.; Dobash, P. A. *Chem. Phys.* **1967**, *47*, 2026.
(53) Mack, J.; Stillman, M. J. In *Handbook of Porphyrins and Related Macrocycles*; Kadish, K., Smith, K., Guilard, R., Eds.; Academic Press: New York, 2002; Vol. 16, Chapter 103.
(54) Mack, J.; Stillman, M. J. *Inorg. Chem.* **1997**, *36*, 413.

Table 1. Calculated Electronic Excitation Spectrum of ZnPc(−2) Obtained from the ZINDO Program[3c,e,54]

no.[a]	sym[b]	calcd[c]	obsd[d]	wave function[e]	assignment[f]
1	$^1A_{1g}$				
2, 3	$^1E_{ux}$	14.8 (0.903)	14.8	$-.950\|1e_g^*\leftarrow 1a_{1u}\rangle + .260\|1e_g^*\leftarrow 1a_{2u}\rangle$ +...	Q
6, 7	$^1E_{ux}$	30.0 (0.023)		$-.978\|2e_g^*\leftarrow 1a_{1u}\rangle$+...	2nd $\pi\rightarrow\pi^*$
13	$^1A_{2u}$	34.1 (0.032)	16.5	$.561\|1e_g^*\leftarrow e_u^N\rangle - .472\|1b_{2u}^*\leftarrow b_{1g}^N\rangle$ +...	n $\rightarrow \pi^*$
14, 15	$^1E_{ux}$	34.3 (0.428)	25.5	$.808\|1e_g^*\leftarrow 1b_{1u}\rangle - .255\|1b_{2u}^*\leftarrow 1e_g\rangle - .221\|1e_g^*\leftarrow 1a_{2u}\rangle$+...	B1
16, 17	$^1E_{ux}$	34.7 (2.233)	29.9	$-.815\|1e_g^*\leftarrow 1a_{2u}\rangle - .348\|3e_g^*\leftarrow 1a_{1u}\rangle - .252\|1e_g^*\leftarrow 1b_{1u}\rangle + .228\|1e_g^*\leftarrow 1a_{1u}\rangle$ +...	B2
21, 22	$^1E_{ux}$	36.5 (0.330)	33.6	$-.574\|3e_g^*\leftarrow 1a_{1u}\rangle + .371\|1e_g^*\leftarrow 1a_{2u}\rangle - .259\|1b_{1u}^*\leftarrow 1e_g\rangle - .251\|2e_g^*\leftarrow 2a_{2u}\rangle - .222\|2e_g^*\leftarrow 1b_{1u}\rangle$+...	N
29, 31	$^1E_{ux}$	39.0 (0.014)	36.2	$-.635\|3e_g^*\leftarrow 1a_{1u}\rangle - .593\|1e_g^*\leftarrow 1b_{2u}\rangle + .278\|1e_g^*\leftarrow 2a_{1u}\rangle + .216\|1b_{2u}^*\leftarrow 2e_g\rangle$ +...	L
34, 35	$^1E_{ux}$	41.1 (0.019)	40.7	$-.744\|1e_g^*\leftarrow 2a_{2u}\rangle + .451\|1e_g^*\leftarrow 1b_{1u}\rangle - .293\|1e_g^*\leftarrow 1b_{2u}\rangle + .255\|3e_g^*\leftarrow 1a_{1u}\rangle$ +...	C

[a] The number of the state assigned in terms of ascending energy in the ZINDO calculation. Electronic transitions with a nonzero oscillator strength between 0 and 50000 cm^{-1} are included in the table. [b] The symmetry of the state under D_{4h} symmetry. [c] The calculated band energies (10^3·cm^{-1}) and oscillator strengths in parentheses. [d] Observed energies (10^3·cm^{-1}) from the spectral deconvolution data of Nyokong et al.[31] [e] The calculated wave functions based on the eigenvectors produced by the configuration interaction calculation of the ZINDO program. N denotes MOs associated with the aza-nitrogen lone pair orbitals. The orbital energies are shown in Table 4. [f] The assignment is described in the text.

^{1}H NMR Spectroscopy. Analysis of the NMR of MPc(−2) complexes is based on the assumption that the ^{1}H signal shifts to lower field when there is a stronger ring current.[37,55] In tetra-*tert*-butylated H_2TAP, H_2Pc, H_2Nc, and anthracocyanine, the pyrrole ^{1}H signals were observed at −2.47, −2.17, −1.64, and −0.73 ppm in $CDCl_3$, respectively, because of the impact of ring expansion.[19a,56] Reduction of the molecular symmetry from D_{4h} to either C_{2v}(III) or D_{2h} through the addition of peripheral fused benzene rings to MPc(−2) should therefore reduce the strength of the ring current of the inner cyclic polyene.[57] The anticipated shift of protons a and b to higher field can be seen in the NMR spectra of ZnPc(−2), Zn3B1N, Zncis2B2N, and Zn3BoN, and for protons c, d, and e in the spectra of Nc(−2) and Zn1B3N, Figure 2. When the π-system of the peripheral benzene rings in ZnPc(−2) is extended through the addition of naphthalene rings to form ZnNc(−2), the signal of proton b shifts to slightly higher field. The signals of protons a, c, and d do not appear to change appreciably as the number of naphthalene units is increased in the Zn3B1N, Zncis2B2N, and Zn1B3N series of C_{2v}(III) complexes (the signals of protons c and c′ split significantly in the case of Zncis2B2N and Zn1B3N). There is an abrupt shift to lower field in the signals of c, d, and e of Zntrans2B2N, which has D_{2h} rather than C_{2v}(III) symmetry, relative to those observed for the D_{4h} ZnNc(−2) complex. In contrast, the signals of protons a and b are approximately the same as those in ZnPc(−2). Proton k of Zn3BoN sits at significantly lower field, because of the close proximity of one of the aza-nitrogens of the inner

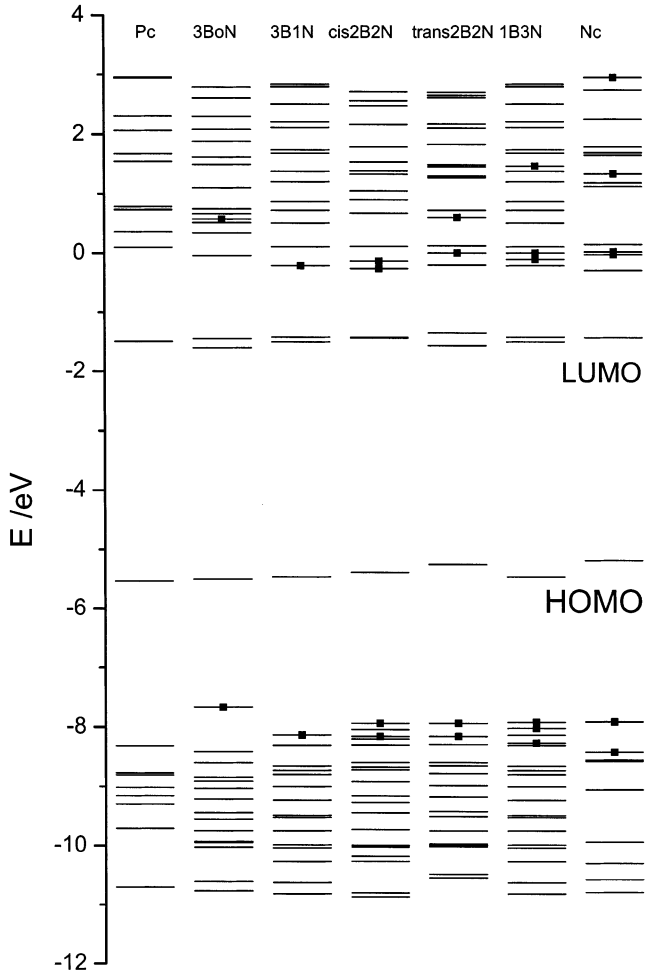

Figure 4. Energy of the π-system MOs predicted by INDO/1 calculations for ZnPc(−2) (Pc), Zn3BoN, Zn3B1N, Zncis2B2N, Zntrans2B2N, and ZnNc(−2), Tables 4 and 5. Additional MOs associated primarily with the peripheral fused naphthalene units are indicated with a square.

(55) (a) Esposito, J. N.; Sutton, L. E.; Kenney, M. E. *Inorg. Chem.* **1967**, *6*, 1116. (b) Janson, T. R.; Kane, A. R.; Sullivan, J. F.; Knox, K.; Kenney, M. E. *J. Am. Chem. Soc.* **1969**, *91*, 5210; **1972**, *94*, 2132. (d) Koyama, T.; Suzuki, T.; Hanabusa, K.; Shirai, H.; Kobayashi, N. *Inorg. Chim. Acta* **1994**, *218*, 41.
(56) Kobayashi, N. Unpublished data.
(57) Kobayashi, N.; Togashi, M.; Osa, T.; Ishii, K.; Yamauchi, S.; Hino, H. *J. Am. Chem. Soc.* **1996**, *118*, 1073.

Table 2. Electronic Excitation Spectrum of Zn3BoN Obtained from the ZINDO Program[a]

no.[b]	sym[c]	calcd[d]	obsd[e]	wave function[f]	assignment[g]
1	A′				ground state
2	A′	14.5 (0.977)	14.7	−**.952**|**1a"*←1a"**⟩**....**	$1a_{1u} \rightarrow 1e_g^*$ (Q)
3	A′	15.2 (0.803)	15.1	−**.945**|**2a"*←1a"**⟩+**....**	$1a_{1u} \rightarrow 1e_g^*$ (Q)
6	A′	27.8 (0.133)		−.754|2a"*←2a"⟩+*.493*|*4a"*←1a"*⟩+....	RN → CP
8	A′	30.4 (0.316)		.604|2a"*←2a"⟩+**.426**|**7a"*←1a"**⟩− **.382**|**6a"*←1a"**⟩+.367|5a"*←1a"⟩+....	RN → CP
9	A′	30.7 (0.380)		−**.725**|**6a"*←1a"**⟩−.550|2a"*←2a"⟩− *.250*|*9a"*←1a"*⟩+....	$1a_{1u} \rightarrow 2e_g^*$ (2nd $\pi \rightarrow \pi^*$)
11	A"	31.9 (0.005)		.678|1a′*←1a′^{N}⟩+.447|2a"*←1a′^{N}⟩− .260|3a"*←1a′^{N}⟩−.254|2a"*←3a′⟩+....	n → π^*
12	A"	32.6 (0.001)		−.674|2a′*←1a′^{N}⟩+.407|1a"*←1a′^{N}⟩+ .296|1a"*←3a′^{N}⟩−.211|2a"*←3a′^{N}⟩+....	n → π^*
13	A′	32.9 (0.353)		*.612*|*8a"*←1a"*⟩+*.354*|*1a"*←4a"*⟩− .276|2a"*←2a"⟩−*.214*|*2a"*←5a"*⟩− .206|7a"*←2a"⟩+**.201**|**3a"*←4a"**⟩+....	new "parity forbidden"
14	A′	33.4 (0.339)	25.6	−**.673**|**1a"*←6a"**⟩+*.430*|*2a"*←5a"*⟩+ **.358**|**1a"*←9a"**⟩−**.267**|**1a"*←3a"**⟩− *.200*|*3a"*←9a"*⟩+....	$1b_{1u} \rightarrow 1e_g^*$ (B2)
16	A′	34.0 (2.032)	27.1	−**.713**|**1a"*←3a"**⟩−*.353*|*1a"*←4a"*⟩+ *.283*|*1a"*←6a"*⟩+**.242**|**10a"*←1a"**⟩+ **.239**|**2a"*←1a"**⟩−.232|1a"*←2a"⟩+....	$1a_{2u} \rightarrow 1e_g^*$ (B1)
18	A′	34.6 (0.581)	28.1	−**.487**|**2a"*←3a"**⟩−**.432**|**2a"*←6a"**⟩+ *.363*|*1a"*←5a"*⟩+*.267*|*9a"*←1a"*⟩− *.214*|*2a"*←4a"*⟩+....	$1a_{2u} \rightarrow 1e_g^*$ (B1)
19	A′	34.7 (0.267)		*.538*|*8a"*←1a"*⟩−*.504*|*1a"*←4a"*⟩+ **.303**|**1a"*←3a"**⟩−**.261**|**2a"*←3a"**⟩+ **.202**|**3a"*←4a"**⟩+....	new "parity forbidden"
20	A′	36.0 (0.228)	29.6	**.578**|**2a"*←6a"**⟩+**.339**|**2a"*←9a"**⟩+ *.278*|*2a"*←7a"*⟩+*.215*|*9a"*←1a"*⟩− **.208**|**3a"*←5a"**⟩+....	$1b_{1u} \rightarrow 1e_g^*$ (B2)
21	A′	36.2 (0.538)	30.8	**.407**|**2a"*←3a"**⟩+.385|9a"*←2a"⟩− *.327*|*1a"*←8a"*⟩−*.257*|*4a"*←6a"*⟩+ **.206**|**2a"*←9a"**⟩+....	B1/rN → CP
22	A′	36.3 (0.122)		**.506**|**10a"*←1a"**⟩+**.272**|**1a"*←9a"**⟩− **.234**|**4a"*←5a"**⟩−*.229*|*2a"*←8a"*⟩− *.227*|*1a"*←7a"*⟩+**.222**|**1a"*←3a"**⟩− **.203**|**2a"*←10a"**⟩+....	$1a_{1u} \rightarrow 3e_g^*$
23	A′	36.4 (0.515)		*.399*|*2a"*←7a"*⟩−*.393*|*1a"*←8a"*⟩+ *.360*|*1a"*←5a"*⟩+**.360**|**2a"*←3a"**⟩+ *.287*|*8a"*←1a"*⟩−**.206**|**2a"*←9a"**⟩+....	new "parity forbidden"
35	A′	40.3 (0.136)		−**.454**|**1a"*←9a"**⟩+**.387**|**10a"*←1a"**⟩ −*.358*|*1a"*←7a"*⟩+*.309*|*2a"*←4a"*⟩− *.302*|*8a"*←1a"*⟩−**.238**|**1a"*←6a"**⟩+ *.234*|*4a"*←10a"*⟩+....	$2a_{2u} \rightarrow 1e_g^*$
52	A′	45.7 (0.107)		**.856**|**14a"*←1a"**⟩+.387|17a"*←1a"⟩+....	$1a_{1u} \rightarrow 4e_g^*$
53	A′	46.2 (0.131)		−*.723*|*16a"*←1a"*⟩−**.387**|**15a"*←1a"**⟩ −**.288**|**1a"*←11a"**⟩−**.275**|**2a"*←10a"**⟩ +....	new "parity forbidden"
56	A′	47.1 (0.179)		−*.617*|*3a"*←3a"*⟩−**.213**|**1a"*←11a"**⟩ +....	new "parity forbidden"
58	A′	47.4 (0.611)		−**.413**|**1a"*←11a"**⟩+.407|4a"*←2a"⟩ −**.267**|**14a"*←1a"**⟩+**.254**|**3a"*←4a"**⟩ +.245|5a"*←4a"⟩+....	$1b_{2u} \rightarrow 1e_g^*$
59	A′	48.0 (0.145)		**.428**|**2a"*←10a"**⟩−*.398*|*3a"*←3a"*⟩ −**.212**|**15a"*←1a"**⟩−*.211*|*16a"*←1a"*⟩ +.208|5a"*←3a"⟩+....	$2a_{1u} \rightarrow 1e_g^*$
60	A′	48.7 (0.145)		−.518|4a"*←2a"⟩+.407|5a"*←2a"⟩ −.268|7a"*←2a"⟩+.239|8a"*←2a"⟩ +*.229*|*4a"*←3a"*⟩+....	RN → CP
61	A′	49.2 (0.197)		−**.495**|**2a"*←11a"**⟩+*.317*|*4a"*←3a"*⟩ −**.307**|**3a"*←4a"**⟩+.257|5a"*←4a"⟩ −.221|5a"*←3a"⟩−*.214*|*3a"*←3a"*⟩+....	$1b_{2u} \rightarrow 1e_g^*$/new "parity forbidden"
62	A′	49.7 (0.442)		−**.459**|**2a"*←11a"**⟩+*.271*|*1a"*←13a"*⟩ +**.208**|**3a"*←4a"**⟩−*.207*|*1a"*←12a"*⟩ −.201|17a"*←1a"⟩+.201|13a"*←2a"⟩ +....	$1b_{2u} \rightarrow 1e_g^*$

[a] The energies of the molecular orbitals are shown in Tables 4 and 5, and spectral deconvolution parameters are reported in Tables S4 and S9. [b] The number of the state assigned in terms of ascending energy in the ZINDO calculation. All electronic transitions with an oscillator strength of greater than 0.1 between 0 and 50000 cm^{-1} are included in the table. [c] The symmetry of the state assuming C_s molecular symmetry. [d] The calculated band energies ($10^3 \cdot cm^{-1}$) and oscillator strengths in parentheses. [e] The band center energies ($10^3 \cdot cm^{-1}$) and intensities obtained from spectral deconvolution analysis are reported in Tables S4 and S9. [f] The calculated wave functions based on the eigenvectors produced by the configuration interaction calculation of the ZINDO program.[47] N denotes MOs associated with the aza-nitrogen lone pair orbitals. One-electron transitions shown in bold and italic are parity allowed and forbidden, respectively, in terms of the corresponding orbitals of ZnPc(−2) under D_{4h} symmetry, Table 4. One-electron transitions that are underlined involve orbitals that are associated primarily with the new peripheral fused-ring extension to the π-system. [g] The assignment is based on the orbitals of ZnPc(−2) with the corresponding nodal and antinodal pattern, Tables 4 and 5.

Table 3. Electronic Excitation Spectrum of Zntrans2B2N Obtained from the ZINDO Program[a]

no.[b]	sym[c]	calcd[d]	obsd[e]	wave function[f]	assignment[g]
1	A_g				ground state
2	B_{2u}	13.8 (0.956)	13.7	$-.957\|1b_{2g}{}^{*}\leftarrow 1a_u\rangle+$....	$1a_{1u}\rightarrow 1e_g{}^{*}$ (Q)
3	B_{3u}	14.5 (1.184)	14.4	$-.954\|1b_{3g}{}^{*}\leftarrow 1a_u\rangle+$....	$1a_{1u}\rightarrow 1e_g{}^{*}$ (Q)
10	B_{3u}	31.8 (0.377)		$-.573\|1b_{3g}{}^{*}\leftarrow 2a_u\rangle-.436\|3b_{3g}{}^{*}\leftarrow 1a_u\rangle+$ $.282\|1a_u{}^{*}\leftarrow 1b_{3g}\rangle-.270\|1b_{1u}{}^{*}\leftarrow 1b_{2g}\rangle+$ $.262\|1b_{2g}{}^{*}\leftarrow 2b_{1u}\rangle+.220\|1b_{2g}{}^{*}\leftarrow 1b_{1u}\rangle+$....	2N → CP
12	B_{3u}	33.4 (2.774)	26.2	$.709\|1b_{2g}{}^{*}\leftarrow 1b_{1u}\rangle-.379\|1b_{2g}{}^{*}\leftarrow 2b_{1u}\rangle-$ $.373\|1b_{2g}{}^{*}\leftarrow 3b_{1u}\rangle+0.274\|1b_{1u}{}^{*}\leftarrow 1b_{2g}\rangle$ +....	$1a_{2u}\rightarrow 1e_g{}^{*}$ (B1)
17	B_{3u}	34.4 (0.707)	27.6	$-.603\|1b_{2g}{}^{*}\leftarrow 2b_{1u}\rangle-.472\|1b_{2g}{}^{*}\leftarrow 3b_{1u}\rangle-$ $.461\|1b_{2g}{}^{*}\leftarrow 1b_{1u}\rangle+.227\|1a_u{}^{*}\leftarrow 2b_{3g}\rangle$ +....	$1b_{1u}\rightarrow 1e_g{}^{*}$ (B2)
20	B_{2u}	34.8 (0.767)	28.8	$-.718\|3b_{2g}{}^{*}\leftarrow 1a_u\rangle-.328\|1b_{3g}{}^{*}\leftarrow 1b_{1u}\rangle+$ $.319\|4b_{2g}{}^{*}\leftarrow 1a_u\rangle-.281\|1b_{3g}{}^{*}\leftarrow 3b_{1u}\rangle-$ $.236\|1b_{2\,g}{}^{*}\leftarrow 2a_u\rangle+$....	$1a_{1u}\rightarrow 2e_g{}^{*}$ (2nd $\pi\rightarrow\pi^{*}$)
22	B_{1u}	35.3 (0.028)		$.650\|1b_{2g}{}^{*}\leftarrow 1b_{2u}{}^{N}\rangle+.468\|1b_{3g}{}^{*}\leftarrow 1b_{3u}{}^{N}\rangle+$ $.383\|1a_u{}^{*}\leftarrow 1b_{1g}{}^{N}\rangle+$....	$n\rightarrow\pi^{*}$
23	B_{2u}	35.6 (0.924)	30.0	$-.726\|1b_{3g}{}^{*}\leftarrow 2b_{1u}\rangle+.348\|1b_{2\,g}{}^{*}\leftarrow 2a_u\rangle-$ $.311\|1b_{3g}{}^{*}\leftarrow 1b_{1u}\rangle+$....	$1b_{1u}\rightarrow 1e_g{}^{*}$ (B2)
25	B_{2u}	36.0 (0.648)	31.5	$.724\|1b_{3g}{}^{*}\leftarrow 1b_{1u}\rangle+.337\|1b_{2g}{}^{*}\leftarrow 2a_u\rangle-$ $.278\|1b_{3g}{}^{*}\leftarrow 2b_{1u}\rangle+.224\|1b_{2g}{}^{*}\leftarrow 1a_u\rangle+$....	$1a_{2u}\rightarrow 1e_g{}^{*}$ (B1)
32	B_{1u}	39.0 (0.004)		$-.695\|1b_{3g}{}^{*}\leftarrow 1b_{3u}{}^{N}\rangle+.616\|1b_{2g}{}^{*}\leftarrow 1b_{2u}{}^{N}\rangle$ +....	$n\rightarrow\pi^{*}$
33	B_{2u}	39.2 (0.475)	32.8	$-.663\|4b_{2g}{}^{*}\leftarrow 1a_u\rangle-.458\|1b_{2g}{}^{*}\leftarrow 3a_u\rangle-$ $.312\|1b_{1u}{}^{*}\leftarrow 1b_{3g}\rangle-.295\|2b_{2g}{}^{*}\leftarrow 2a_u\rangle$ $-.252\|1b_{3g}{}^{*}\leftarrow 1b_{1u}\rangle+$....	$1a_{1u}\rightarrow 3e_g{}^{*}$
42	B_{2u}	41.2 (0.723)		$-.553\|1b_{1u}{}^{*}\leftarrow 1b_{3g}\rangle+.471\|2b_{2g}{}^{*}\leftarrow 2a_u\rangle-$ $.384\|4b_{2g}{}^{*}\leftarrow 1a_u\rangle-.258\|2b_{2g}{}^{*}\leftarrow 2a_u\rangle+$....	2N → CP
56	B_{3u}	46.9 (1.134)		$-.408\|1a_u{}^{*}\leftarrow 1b_{3g}\rangle-.396\|1b_{1u}{}^{*}\leftarrow 1b_{2g}\rangle+$ $.294\|3b_{1u}{}^{*}\leftarrow 1b_{2g}\rangle-.242\|2b_{2g}{}^{*}\leftarrow 2b_{1u}\rangle-$ $.238\|3b_{3g}{}^{*}\leftarrow 2a_u\rangle+.227\|2b_{2g}{}^{*}\leftarrow 1b_{1u}\rangle+$....	2N → CP
59	B_{2u}	47.4 (0.280)		$.581\|1b_{2g}{}^{*}\leftarrow 3a_u\rangle-.367\|2b_{1u}{}^{*}\leftarrow 2b_{3g}\rangle+$ $.280\|2b_{3g}{}^{*}\leftarrow 2b_{1u}\rangle+.280\|4b_{2g}{}^{*}\leftarrow 1a_u\rangle+$ $.252\|2b_{3g}{}^{*}\leftarrow 1b_{1u}\rangle-.217\|1b_{3g}{}^{*}\leftarrow 1b_{1u}\rangle+$....	$1b_{2u}\rightarrow 1e_g{}^{*}$
63	B_{3u}	48.8 (0.264)		$.603\|2b_{2g}{}^{*}\leftarrow 1b_{1u}\rangle+.367\|2b_{2g}{}^{*}\leftarrow 2b_{1u}\rangle+$ $.293\|1a_u{}^{*}\leftarrow 1b_{3g}\rangle+.259\|1b_{1u}{}^{*}\leftarrow 2b_{2g}\rangle-$ $.238\|2b_{2g}{}^{*}\leftarrow 3b_{1u}\rangle+.223\|1b_{1u}{}^{*}\leftarrow 1b_{2g}\rangle+$....	2N → CP

[a] The energies of the molecular orbitals are shown in Tables 4 and 5, and spectral deconvolution data are reported in Tables S7 and S12. [b] The number of the state assigned in terms of ascending energy in the ZINDO calculation. All electronic transitions with an oscillator strength of greater than 0.1 between 0 and 50000 cm^{-1} are included in the table. [c] The symmetry of the state assuming D_{2h} molecular symmetry. [d] The calculated band energies ($10^3\cdot cm^{-1}$) and oscillator strengths in parentheses. [e] The band center energies ($10^3\cdot cm^{-1}$) and intensities obtained from spectral deconvolution analysis are reported in Tables S7 and S12. [f] The calculated wave functions based on the eigenvectors produced by the configuration interaction calculation of the ZINDO program.[47] N denotes MOs associated with the aza-nitrogen lone pair orbitals. One-electron transitions that are underlined involve orbitals that are associated primarily with the new peripheral fused-ring extension to the π-system. [g] The assignment is based on the orbitals of ZnPc(−2) with the corresponding nodal and antinodal pattern, Tables 4 and 5.

cyclic polyene.[58] To interpret the NMR of reduced symmetry phthalocyanine derivatives, the ring currents associated with the 16-atom inner cyclic polyene, benzene, and naphthalene rings systems clearly all have to be taken into consideration.

Optical Spectroscopy. (a) UV−Vis Absorption, Emission, and MCD Spectroscopy. The UV−vis absorption and MCD spectra of ZnPc, Zn3B1N, Zn3BoN, Zncis2B2N, Zntrans2B2N, Zn1B3N, and ZnNc(−2) are shown in Figures 5 and 6, respectively. The A terms associated with the lowest energy $\pi\rightarrow\pi^{*}$ band of ZnPc and ZnNc(−2) are replaced by two intense, oppositely signed, close-lying B terms in the case of Zn3B1N, Zn3BoN, Zncis2B2N, Zntrans2B2N, and Zn1B3N. Michl[24] has demonstrated that the $-\upsilon e/+\upsilon e$ ordering of the signs of a coupled B term to high energy in reduced symmetry cyclic polyene π-systems is consistent with an A term involving an excited state that has greater orbital angular momentum (OAM) than the ground state if D_{4h} or higher symmetry had been maintained.[24]

The impact of perturbations on the electronic structure of the ideal cyclic polyene running around the inner perimeter of the porphyrin π-system can be predicted qualitatively by considering the location of the nodes and antinodes of the four frontier orbitals by the "Symmetry-adapted Perturbation Method".[18c,19b,23,24,59] The pyrrolic nitrogens lie on a node of the HOMO a_{2u} orbital and are very close to the nodes of the second HOMO a_{1u} orbital of MP(−2). As a result, the addition of pyrrolic nitrogens to the cyclic polyene has almost no impact on the separation between the $1a_{1u}$ and $1a_{2u}$ HOMO orbitals (ΔHOMO) so these two orbitals can be viewed as being essentially degenerate in the case of MP(−2). The addition of the aza-nitrogen bridges and fused benzene rings to form MPc(−2) breaks this accidental degeneracy of the HOMO level. There is, therefore, reduced mixing between the Q and B excited states, and the Q band shifts to the red and gains significant intensity.[36] The expansion of the π-system through the addition of four additional fused

(58) Nonomura, T.; Kobayashi, N.; Tomura, T. *J. Porphyrins Phthalocyanines* **2000**, *4*, 538.

(59) Solovev, K. N.; Mashenkov, V. A.; Kachura, T. F. *Opt. Spectrosc.* **1969**, *27*, 24.

Table 4. Calculated Energies and Symmetries of the π-System MOs of a Model Complex Comprising the Inner Cyclic Polyene Ring of ZnPc (ZnCP), Zinc Tetraazaporphyrin (ZnTAP), ZnPc, Zn3B1N, Zn3BoN, Zncis2B2N, Zntrans2B2N, Zn1B3N, and ZnNPc(−2)[a]

	ZnCP		ZnTAP		ZnPc(−2)		Zn3BoN		Zn3B1N		Zncis2B2N		Zntrans2B2N		Zn1B3N		ZnNPc(−2)	
M_L	D_{4h}	E/eV	D_{4h}	E/eV	D_{4h}	E/eV	C_s	E/eV	C_2v(III)	E/eV	C_2v(III)	E/eV	D_{2h}	E/eV	C_2v(III)	E/eV	D_{4h}	E/eV
					$3b_{2u}$*	3.844	21a"*	3.957	$11a_2$*	3.957	$12b_2$*	4.010	$6a_u$*	4.016	$13a_2$*	4.067	$3b_{2u}$*	4.062
					*$5e_g$**	*3.792*	*20a"**	*3.892*	*$10b_2$**	*3.808*	*$11b_2$**	*3.897*	*$6b_{3g}$**	*4.013*	*$12b_2$**	*4.021*	*$7e_g$**	*4.036*
						3.791	*18a"**	*3.748*	*$10a_2$**	*3.892*	*$11a_2$**	*3.929*	*$6b_{2g}$**	*3.822*	*$11a_2$**	*3.854*		*4.032*
					$2a_{1u}$*	3.678	19a"*	3.808	$9a_2$*	3.748	$10a_2$*	3.852	$5a_u$*	3.788	$12a_2$*	3.981	$3a_{1u}$*	3.992
																	*$6e_g$**	*3.287*
											*$8b_2$**	*2.854*	*$5b_{3g}$**	*3.259*	*$9a_2$**	*3.119*		*3.285*
															$11b_2$*	3.315	$4b_{1u}$*	3.233
8	**$1a_{2u}$***	**2.260**	**$1a_{2u}$***	**2.310**	**$2a_{2u}$***	**2.961**	**16a"***	**3.029**	**$9b_2$***	**3.054**	**$10b_2$***	**3.194**	**$5b_{1u}$***	**2.995**	**$10b_2$***	**2.996**	**$4a_{2u}$***	**3.024**
							17a"*	3.121	$8a_2$*	3.121	$8a_2$*	2.720	$4a_u$*	3.083	$8a_2$*	2.730	$2a_{1u}$*	2.953
±7	***$2e_g$****	***2.385***	***$3e_g$****	***2.694***	***$4e_g$****	***2.945***	***15a"****	***2.850***	***$8b_2$****	***2.903***	***$9b_2$****	***2.989***	***$4b_{3g}$****	***2.710***	***$9b_2$****	***2.756***	***$5e_g$****	***2.749***
		2.385		***2.693***		***2.946***	***14a"****	***2.796***	***$7a_2$****	***2.800***	***$9a_2$****	***3.138***	***$5b_{2g}$****	***2.988***	***$10a_2$****	***3.145***		***2.747***
			$2b_{2u}$*	2.673	$2b_{2u}$*	2.310	13a"*	2.302	$6a_2$*	2.217	$7b_2$*	2.168	$3a_u$*	2.108	$7a_2$*	2.109	$2b_{2u}$*	2.261
					$2b_{1u}$*	2.066	12a"*	2.086	$7b_2$*	2.121	$7a_2$*	2.168	$4b_{1u}$*	2.176	$8b_2$*	2.212	$3b_{1u}$*	1.796
			*$2e_g$**	*1.707*	*$3e_g$**	*1.677*	*11a"**	*1.886*	*$6b_2$**	*1.743*	*$6b_2$**	*1.539*	*$3b_{3g}$**	*1.299*	*$6b_2$**	*1.469*	*$4e_g$**	*1.697*
				1.704		*1.676*	*10a"**	*1.619*	*$4a_2$**	*1.205*	*$6a_2$**	*1.794*	*$4b_{2g}$**	*1.832*	*$6a_2$**	*1.665*		*1.693*
															$7b_2$*	1.558	$2b_{1u}$*	1.338
			$1a_{1u}$*	1.975	$1a_{1u}$*	1.544	9a"*	1.497	$5a_2$*	1.689	$5a_2$*	1.392	$2a_u$*	1.280	$5a_2$*	1.437	$1a_{1u}$*	1.124
					$1a_{2u}$*	0.787	8a"*	1.101	$5b_2$*	1.380	$5b_2$*	1.331	$3b_{1u}$*	1.488	$5b_2$*	1.176	$2a_{2u}$*	1.651
					*$2e_g$**	*0.736*	*7a"**	*0.749*	*$4b_2$**	*0.874*	*$4b_2$**	*0.907*	*$2b_{3g}$**	*1.457*	*$4b_2$**	*0.831*	*$3e_g$**	*1.189*
						0.734	*6a"**	*0.667*	*$3a_2$**	*0.729*	*$4a_2$**	*1.050*	*$3b_{2g}$**	*0.728*	*$4a_2$**	*1.052*		*1.189*
																	*$2e_g$**	*0.023*
											*$2a_2$**	*−0.259*	*$2b_{2g}$**	*0.001*	*$2a_2$**	*0.001*		*0.019*
							*5a"**	*0.573*	$2b_2$*	−0.208	$2b_2$*	−0.130	$2b_{1u}$*	−0.199	*$3b_2$**	*−0.102*	$1a_{2u}$*	*−0.024*
±6	**$1b_{2u}$***	**1.644**	**$1b_{2u}$***	**1.180**	**$1b_{2u}$***	**0.098**	**4a"***	**0.337**	**$3b_2$***	**0.507**	**$3a_2$***	**0.678**	**$2b_{1u}$***	**0.505**	**$2b_2$***	**−0.283**	**$1b_{1u}$***	**0.147**
	$1b_{1u}$*	**0.763**	**$1b_{1u}$***	**−0.266**	**$1b_{1u}$***	**0.359**	**3a"***	**−0.041**	**$2a_2$***	**0.107**	**$3b_2$***	**0.115**	**$1a_u$***	**0.125**	**$3a_2$***	**0.140**	**$1b_{2u}$***	**−0.295**
±5	***$1e_g$****	***−0.989***	***$1e_g$****	***−1.843***	***$1e_g$****	***−1.495***	***2a"****	***−1.447***	***$1b_2$****	***−1.415***	***$1b_2$****	***−1.423***	***$1b_{3g}$****	***−1.348***	***$1b_2$****	***−1.349***	***$1e_g$****	***−1.426***
		−0.987		***−1.842***		***−1.493***	***1a"****	***−1.603***	***$1a_2$****	***−1.504***	***$1a_2$****	***−1.434***	***$1b_{2g}$****	***−1.563***	***$1a_2$****	***−1.479***		***−1.426***
±4	**$1a_{1u}$**	**−5.328**	**$1a_{1u}$**	**−6.264**	**$1a_{1u}$**	**−5.534**	**1a"**	**−5.600**	**$1a_2$**	**−5.459**	**$1a_2$**	**−5.389**	**$1a_u$**	**−5.353**	**$1a_2$**	**−5.292**	**$1a_{1u}$**	**−5.183**
	$1a_{2u}$	**−8.431**	**$1a_{2u}$**	**−8.365**	**$1a_{2u}$**	**−8.318**	**3a"**	**−8.413**	**$1b_2$**	**−8.305**	**$2b_2$**	**−8.298**	**$1b_{1u}$**	**−8.289**	**$2b_2$**	**−8.280**	**$1a_{2u}$**	**−7.908**
							2a"	**−7.665**	**$2a_2$**	**−8.134**	**$1b_2$**	**−8.044**	**$2a_u$**	**−8.153**	**$2a_2$**	**−8.018**	**$1b_{2u}$**	**−7.908**
																	$1e_g$	*−7.914*
											$2a_2$	*−8.202*	*$1b_{3g}$*	*−7.937*	*$1b_2$*	*−7.921*		*−7.915*
															$3a_2$	*−8.268*	$2a_{1u}$	−8.417
			$1b_{1u}$	−9.211	$1b_{1u}$	−8.780	6a"	−8.911	$2b_2$	−8.658	$4a_2$	−8.719	$2b_{1u}$	−8.652	$3b_2$	−8.534	$1b_{1u}$	−8.551
			$1e_g$	*−9.241*	*$1e_g$*	*−8.811*	*4a"*	*−8.603*	*$3b_2$*	*−8.735*	*$3b_2$*	*−8.675*	*$2b_{3g}$*	*−8.782*	*$4b_2$*	*−8.704*	*$2e_g$*	*−8.573*
				−9.246		*−8.813*	*5a"*	*−8.843*	*$3a_2$*	*−8.802*	*$3a_2$*	*−8.596*	*$1b_{2g}$*	*−8.598*	*$4a_2$*	*−8.594*		*−8.578*
					$2e_g$	*−9.021*	*7a"*	*−9.037*	*$4b_2$*	*−9.001*	*$6b_2$*	*−10.167*	*$3b_{3g}$*	*−9.989*	*$6b_2$*	*−9.962*	*$3e_g$*	*−9.933*
						−9.021	*8a"*	*−9.215*	*$6a_2$*	*−10.263*	*$6a_2$*	*−10.261*	*$2b_{2g}$*	*−8.897*	*$6a_2$*	*−10.183*		*−9.933*
					$1b_{2u}$	−9.161	11a"	−9.928	$4a_2$	−9.000	$4b_2$	−8.918	$3a_u$	−9.421	$5a_2$	−9.076	$2b_{2u}$	−10.296
			$2a_{2u}$	−9.765	$2a_{2u}$	−9.297	9a"	−9.284	$5b_2$	−9.233	$5b_2$	−9.158	$3b_{1u}$	−9.178	$5b_2$	−9.110	$2a_{2u}$	−9.053
					$2a_{1u}$	−9.711	10a"		$5a_2$	−9.526	$5a_2$	−9.274	$4a_u$	−10.478	$7a_2$	−10.440	$3a_{1u}$	−10.563
±3	***$1e_g$***	***−10.390***	***$2e_g$***	***−10.399***	***$3e_g$***	***−10.695***	***12a"***	***−10.600***	***$6b_2$***	***−10.619***	***$7b_2$***	***−10.793***	***$4b_{3g}$***	***−10.932***	***$7b_2$***	***−10.858***	***$4e_g$***	***−10.779***
	$1e_g$	***−10.392***		***−10.401***		***−10.698***	***13a"***	***−10.758***	***$7a_2$***	***−10.893***	***$7a_2$***	***−10.872***	***$3b_{2g}$***	***−10.538***	***$8a_2$***	***−10.811***		***−10.783***
															$8b_2$	−11.283	$2b_{1u}$	−11.138
							14a"	−11.583	$7b_2$	−11.614	$8b_2$	−11.825	$4b_{1u}$	−11.369	$9b_2$	−11.819	$3a_{2u}$	−11.678
																	$5e_g$	*−11.712*
											$8a_2$	−11.470	*$5b_{2g}$*	−11.713	$9a_2$	−11.710		−11.715
±2	**$1b_{2u}$**	**−12.730**	**$1b_{2u}$**	**−12.782**	**$2b_{2u}$**	**−12.275**	**16a"**	**−12.875**	**$8a_2$**	**−12.854**	**$9b_2$**	**−12.845**	**$5a_u$**	**−12.869**	**$10a_2$**	**−12.883**	**$3b_{2u}$**	**−12.852**
	$1b_{1u}$	**−13.063**	**$2b_{1u}$**	**−13.670**	**$2b_{1u}$**	**−12.870**	**15a"**	**−12.517**	**$8b_2$**	**−12.469**	**$9a_2$**	**−12.565**	**$5b_{1u}$**	**−12.720**	**$10b_2$**	**−12.693**	**$3b_{1u}$**	**−13.709**
					$4e_g$	*−13.088*	*17a"*	*−13.124*	*$9b_2$*	*−13.087*	*$10b_2$*	*−13.018*	*$6b_{3g}$*	*−14.432*	*$11b_2$*	*−13.964*	*$6e_g$*	*−14.410*
						−13.089	*18a"*	*−13.336*	*$9a_2$*	*−13.115*	*$10a_2$*	*−14.163*	*$6b_{2g}$*	*−13.602*	*$11a_2$*	*−14.427*		*−14.411*
					$3a_{2u}$	−13.292	19a"	−14.070	$10b_2$	−14.420	$11b_2$	−14.665	$6b_{1u}$	−14.240	$12b_2$	−14.686	$4a_{2u}$	−14.847
					$3b_{1u}$	−15.157	20a"	−15.289	$11b_2$	−15.270	$11a_2$	−15.327	$7b_{1u}$	−15.401	$13b_2$	−15.419	$4b_{1u}$	−15.532
±1	***$2e_g$***	***−14.898***	***$3e_g$***	***−15.040***	***$5e_g$***	***−16.085***	***21a"***	***−16.110***	***$10a_2$***	***−16.070***	***$12a_2$***	***−16.091***	***$7b_{2g}$***	***−16.21***	***$12a_2$***	***−16.197***	***$7e_g$***	***−16.173***
		−14.898		***−15.046***		***−16.086***	***22a"***	***−16.153***	***$12b_2$***	***−16.149***	***$12b_2$***	***−16.176***	***$6b_{3g}$***	***−16.052***	***$14b_2$***	***−16.174***		***−16.175***
0	**$2a_{2u}$**	**−16.256**	**$3a_{2u}$**	**−16.151**	**$4a_{2u}$**	**−17.101**	**23a"**	**−17.132**	**$13b_2$**	**−17.111**	**$13a_2$**	**−17.118**	**$8b_{1u}$**	**−17.104**	**$15b_2$**	**−17.124**	**$5a_{2u}$**	**−17.102**

[a] The rows are ordered according to the nodal and antinodal patterns that are observed for each complex relative to the high symmetry ZnPc(−2) parent complex. The orbital angular momentum associated with the orbitals of the inner cyclic polyene model complex are shown in the left-hand column. The orbitals with the corresponding nodal patterns are highlighted in bold. Italics are used to indicate degenerate orbitals under D_{4h} symmetry.

benzenes to form Nc(−2) results in a further increase in Q band intensity and a further red shift of the Q band center.[60] As would be expected, the A_1/D_0 ratio obtained from MCD spectroscopy decreases on going from ZnPc(−2) to ZnNc(−2) as the separation between the $1a_{1u}$ and $1a_{2u}$ levels increases. The energy differences of the Q band center of ZnPc(−2) and Zncis2B2N (934 cm^{-1}) and that of Zncis2B2N and ZnNc(−2) (876 cm^{-1}) are reasonably similar, Figure 5. There is a slight red shift of the Q bands of Zn3B1N at 682 and 697 nm, relative to that of ZnPc(−2) at 670 nm,[3a] Table 4. In contrast, there is a slight blue shift of the Q band components of Zn1B3N at 725 and 743 nm (using the MCD B term band centers) relative to the Q band of ZnNc(−2) at 750 nm.[3a]

The ZINDO calculations successfully predict the magnitude of the energy gap between the LUMO and HOMO and the associated red shift of the Q band as naphthalene groups are added to the Pc ring, Figure 4. The predicted splitting of

(60) Kobayashi, N.; Nakijima, S.; Osa, T. *Inorg. Chim. Acta* **1993**, *210*, 131.

Table 5. Calculated Energies and Symmetries of the Primarily Aza-Bridging and Pyrrole Nitrogen Lone Pair Based σ-MOs in the −11 to 3 eV Range for a Model Complex Comprising the Inner Cyclic Polyene Ring of ZnPc (ZnCP), Zinc Tetraazaporphyrin (ZnTAP), ZnPc, Zn3B1N, Zn3BoN, Zncis2B2N, Zntrans2B2N, Zn1B3N, and ZnNPc(−2)[a]

ZnPc(−2) D_{4h}		Zn3BoN C_s		Zn3B1N C_2v(III)		Zncis2B2N C_2v(III)		Zntrans2B2N D_{2h}		Zn1B3N C_2v(III)		ZnNPc(−2) D_{4h}	
$1b_{1g}$	−9.532	1a′	−9.445	$1b_1$	−9.493	$1a_1$	−9.447	$1b_{1g}$	−9.493	$1b_1$	−9.411	$1b_{1g}$	−9.488
$1b_{2g}$	−9.766	2a′	−9.750	$1a_1$	−9.746	$1b_1$	−9.728	$1a_u$	−9.746	$1a_1$	−9.739	$1b_{2g}$	−9.759
$1e_u$	*−10.013*	*3a′*	*−9.945*	*$2a_1$*	*−9.983*	*$2b_1$*	*−9.988*	*$2b_{3u}$*	*−9.983*	*$2a_1$*	*−9.948*	*$1e_u$*	*−9.958*
$1e_u$	*−10.018*	*4a′*	*−10.025*	*$2b_1$*	*−10.035*	*$2b_1$*	*−10.017*	*$2b_{2u}$*	*−10.035*	*$2b_1$*	*−10.001*	*$1e_u$*	*−9.958*
$1a_{1g}$	−10.817	5a′	−10.713	$3a_1$	−10.831	$3a_1$	−10.863	$1a_g$	−10.493	$3a_1$	−10.780	$1a_{1g}$	−10.740

[a] The rows are ordered according to the nodal and antinodal patterns that are observed for each complex relative to the high symmetry ZnPc(−2) parent complex. Italics are used to indicate degenerate orbitals under D_{4h} symmetry.

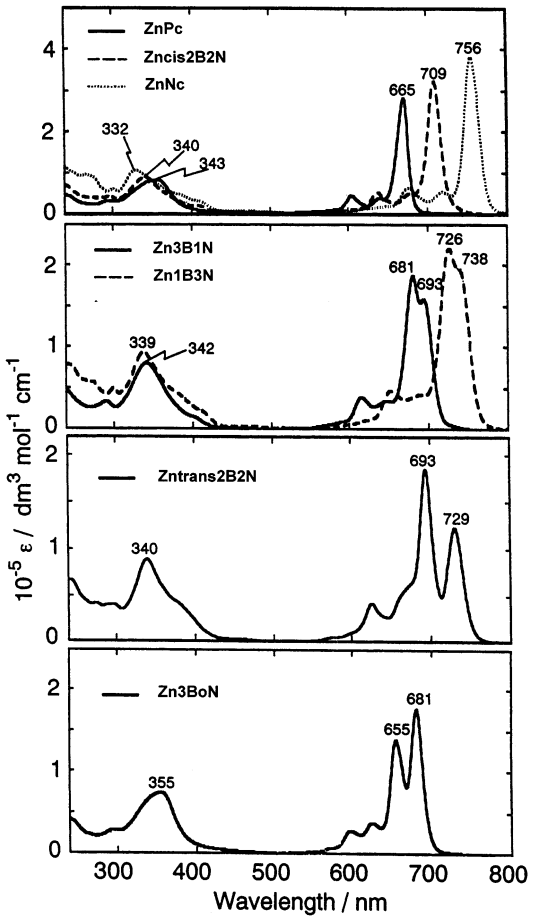

Figure 5. Electronic absorption spectra of ZnPc(−2) **1**, Zn3B1N **2**, Zncis2B2N **3**, Zntrans2B2N **4**, Zn1B3N **5**, ZnNc(−2) **6**, and Zn3BoN **7** in THF.

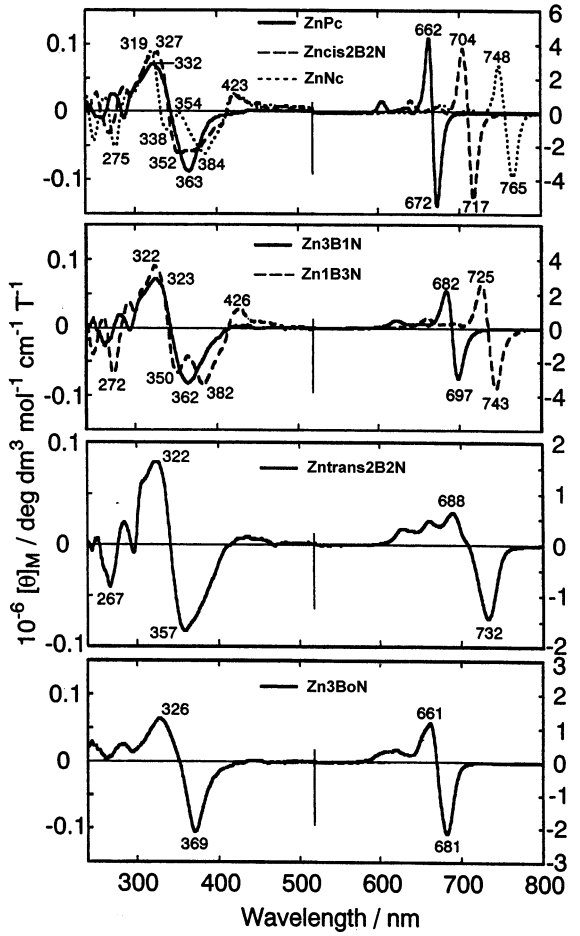

Figure 6. MCD spectra of ZnPc(−2) **1**, Zn3B1N **2**, Zncis2B2N **3**, Zntrans2B2N **4**, Zn1B3N **5**, ZnNc(−2) **6**, and Zn3BoN **7** in THF.

the two Q band components also closely matches the experimental values, Figure 7. The splitting observed in the Q bands of Zntrans2B2N at 688 and 732 nm is significantly greater than is the case with Zncis2B2N where bands are observed at 704 and 717 nm despite the fact that the Zntrans2B2N complex is the higher symmetry complex. The perturbation to the structure of ZnPc(−2) results in different ring substitution patterns along the *x*- and *y*-axes in the case of the D_{2h} Zntrans2B2N isomer while the structure is identical along the *x*- and *y*-axes in the case of Zncis2B2N, Figure 2. The spectrum in the Q region of Zncis2B2N is therefore very similar to that of ZnPc(−2) and ZnNc(−2) as the Q bands of the C_{2v}(III) Zncis2B2N isomer form a pseudo-A term because the excited states associated with the $1a_2 \rightarrow 1a_2^*$ and $1a_2 \rightarrow 1b_2^*$ one-electron transitions are

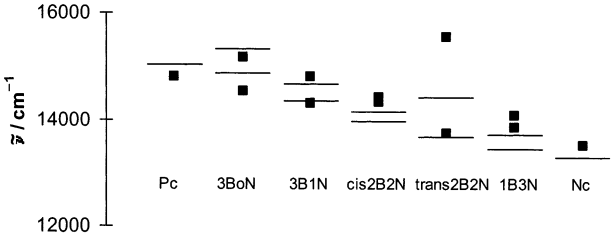

Figure 7. Predicted energies of the Q_{00} bands (−) from ZINDO/s plotted against the experimentally observed values (■) obtained from spectral deconvolution, Tables S4−S8.

nearly degenerate. The spectra of Zn3B1N and Zn3BoN are at first glance very similar to those of ZnPc(−2),[3a,e] but the reduced symmetry results in a slight splitting of the Q band because of the lifting of the orbital degeneracy of the $1e_g^*$

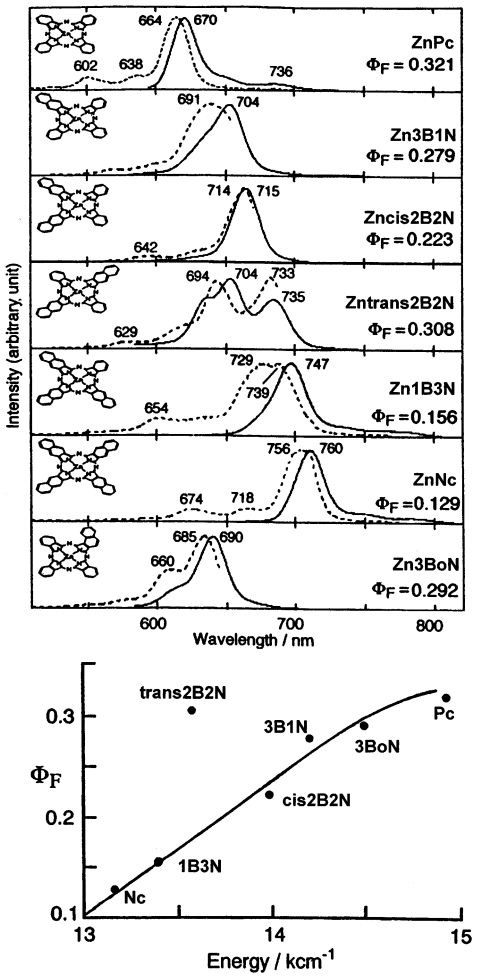

Figure 8. Fluorescence emission and excitation spectra of ZnPc(−2) **1**, Zn3B1N **2**, Zncis2B2N **3**, Zntrans2B2N **4**, Zn1B3N **5**, ZnNc(−2) **6**, and Zn3BoN **7** in deaerated $CHCl_3$.

LUMO. There is a slightly greater splitting between the Q components of Zn3BoN because of the impact of the reduced molecular symmetry, Table 4, but Q band positions of Zn3BoN are closer to that of ZnPc(−2) than is the case with Zn3B1N. These results are consistent with the existing spectral data, which have suggested that oblique substitution or fusion has a relatively minor impact on the wavelength of the Q band.[19a,61] The MCD spectrum of Zn3BoN appears to be almost identical to that of Zn3B1N in the B region while that of Zn1B3N is considerably more complex with significantly greater intensity within the spectral envelope in the 300−450 nm region. Many of the new MOs which result from π-system expansion have energies close to those of the four frontier orbitals of the inner cyclic polyene, Table 4 and Figure 4, so additional one-electron transitions can be expected to contribute to band intensity in this region.

Figure 8 displays the S1 fluorescence emission and excitation spectra of the complexes studied, together with their Φ_F values. The observed Stokes shifts were relatively small in all cases, and Zntrans2B2N is the only complex to show two well-resolved Q bands in the emission and excitation spectra. A deviation from mirror symmetry similar to that reported previously for MPc(−2)[36,62] was observed in the emission and excitation spectra of all the complexes and was particularly marked in the case of the C_{2v}(III) symmetry complexes. When the Φ_F value is plotted against the wavelength of the Q band, Figure 8, a clear linear relationship is observed. This strongly suggests that nonradiative decay becomes easier as the energy gap decreases between the HOMO and the LUMO. The D_{2h} Zntrans2B2N complex where there is the largest energy separation in the *x*- and *y*-polarized Q00 bands represents the only significant outlier from this trend, which indicates that this fused ring substitution pattern has the most profound impact on the electronic properties of the π-system. Emission spectra were recorded at several excitation wavelengths.

(b) Band Deconvolution: The Q and n → π* Spectral Regions. The band deconvolution analyses of the Q region of the absorption and MCD spectra of Zn3BoN, Zn3B1N, Zncis2B2N, Zntrans2B2N, and Zn1B3N provide direct quantitative spectroscopic data on the effect of the asymmetry on the electronic structure, Figures 9 and 10 and Figures S1−S3 (Supporting Information). The two major electronic bands arising from the split Q00 transition are shown in bold. The band deconvolution analysis of spectra obtained on a vitrified ZnPc(−2) solution at cryogenic temperatures, Figure 11, led to the identification of a repeating pattern within the envelope of vibrational bands associated with the Q transition.[36] An a_{1g} vibration combines with the first set of vibrations so that repeating "Q01" and "Q02" envelopes of vibrational bands dominate the spectrum between the Q00 band and the 607 nm band. The energies obtained from our deconvolution analysis for the major vibrational bands were in close agreement with those identified by Huang et al. from fluorescence emission and excitation spectra in low temperature argon matrixes.[62] In the case of ZnPc(−2), a mismatch in the wavelengths of the absorption and MCD bands at ca. 600 nm and the absence of mirror symmetry in the fluorescence and excitation spectra which is not observed in the case of MP(−2) complexes were found to be consistent with a weak n → π* band associated with an MO located primarily on the aza-nitrogen lone pair electrons being the origin for a second weaker set of vibrational bands within the Q spectral envelope.[36,62] The components identified by this deconvolution analysis should be present in the Q spectral region of all phthalocyanine complexes.

A complex envelope of vibrational bands, similar to that observed for MPc(−2), Figure 11, is observed to the blue of the Q band in each of the 5 spectral data sets, Figures 9 and 10 and Figures S1−S3 (Supporting Information). Some minor hot bands associated with the Boltzmann population distribution across the vibrational levels associated with the ground states are observed to the red of the Q band like those observed previously in the case of ZnPc(−2), Figure 12. These hot bands are eliminated in data recorded on vitreous solutions at cryogenic temperatures, Figure 11.[36] Band

(61) Luk'yanets, E. A. *Electronic Spectra of Phthalocyanines and Related Compounds*; NIOPIK: Moscow, 1989.

(62) (a) Huang, T. H.; Rieckhoff, K. E.; Voight, E. M. *J. Chem. Phys.* **1982**, *77*, 3424. (b) Huang, T. H.; Rieckhoff, K. E.; Voight, E. M. *J. Phys. Chem.* **1981**, *85*, 3322.

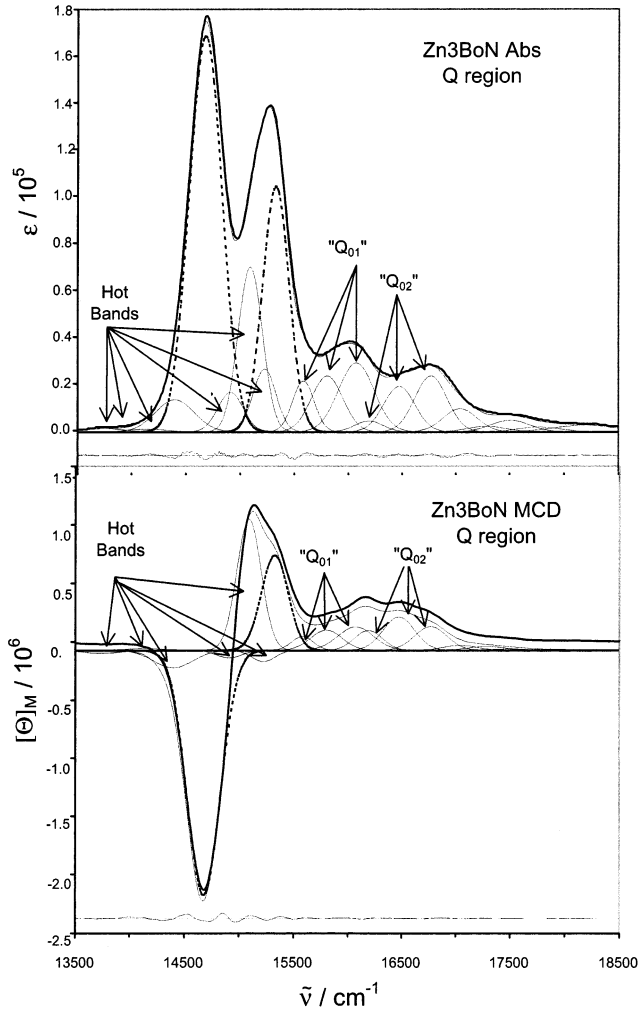

Figure 9. Spectral band deconvolution analysis of the Q spectral region of Zn3BoN. The band fitting parameters can be found in Table S4. Major electronic bands assigned in Table 2 to the Q transition, Figure 3, are shown in bold. The line showing the experimental MCD spectrum has been shifted positive slightly for visual purposes only.

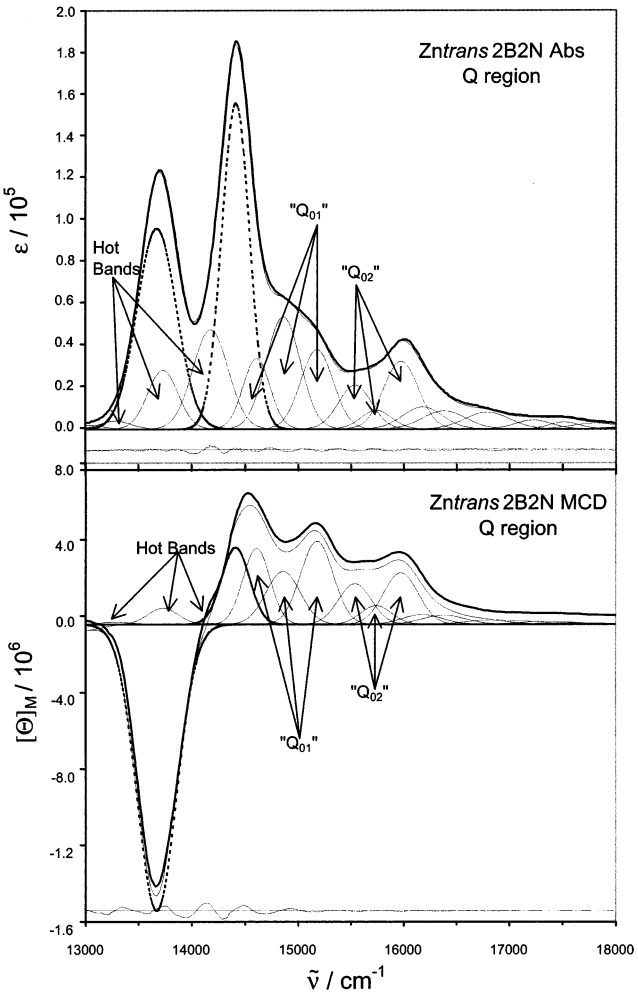

Figure 10. Spectral band deconvolution analysis of the Q spectral region of Zntrans2B2N. The band fitting parameters can be found in Table S7. Major electronic bands assigned in Table 3 to the Q transition, Figure 3, are shown in bold. The line showing the experimental MCD spectrum has been shifted positive slightly for visual purposes only.

broadening due to solvation effects and the splitting of the Q band as a result of reduced symmetry further complicate the spectra and result in a very high degree of band overlap. The rigid shift assumption under which the bandwidths in both the UV−vis and MCD spectra can be assumed to be identical is problematic when hot bands are present.[30] A repeating pattern of "Q01" and "Q02" envelopes can, however, still be seen in the SIMPFIT spectral fits of all five complexes consisting of weak positive overlapping B terms as was observed previously in the case of ZnPc(−2), Figure 11. The analysis provides important new information. The B terms associated with some of the vibrational bands of Zn3BoN and Zntrans2B2N, the complexes where there is the largest splitting of the main Q bands, are more intense than the B term associated with the higher energy component of the symmetry-split Q absorption band, Figures 9 and 10. The higher energy of the symmetry-split Q bands therefore lies to the blue of some of the vibrational bands associated with the lower energy band resulting in a spectrum markedly different from that of ZnPc(−2) because B term intensity is related to the field-induced mixing of close-lying states.

On the blue side of the Q spectral envelope, the calculations identify a set of bands with widths that do not fit the pattern of positive and negative B terms in the "Q01" and "Q02" vibronic progression, Figure 11. These bands are assigned to the weak n → π^* transition observed in the case of ZnPc(−2).[36] There is a significant deviation from mirror symmetry similar to that originally observed by Huang in the fluorescence emission and excitation spectra of ZnPc(−2),[36,62] Figure 8. If this assignment is valid, the ZINDO calculations must significantly underestimate the energy of the σ-MOs based primarily on the aza-nitrogen lone pair orbitals.[54] An MO calculation by Schaffer et al.[28] predicted that the aza-nitrogen lone pair MOs lie in the same energy range as the a_{1u} HOMO orbital while the same MOs lie about 3 eV below the a_{1u} HOMO in a calculation by Henricksson et al.[29a] Unlike the MO calculations, the experimental data obtained from optical spectroscopy are unambiguous and fixed, and the assignment of these bands to a weak n → π^* transition appears to provide the only explanation that can fully account for all the features observed within the spectrum. An anomalous, intense B term in the spectrum of $[MPc(-1)]^+$ at ca. 500 nm to the blue of the Q band in a

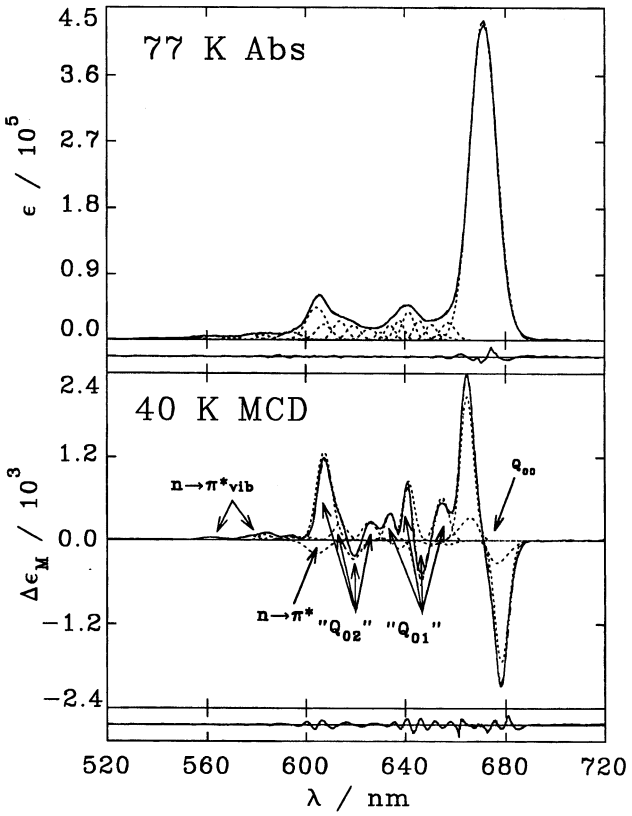

Figure 11. Spectral deconvolution analysis of the Q band region of the absorption and MCD spectra of (CN^-)ZnPc(−2).[36] Identical bandwidths and centers are used to fit the MCD and absorption spectra recorded at 40 and 77 K on a 5:2 dimethyl formamide/dimethyl acetamide vitrified solution. The solid, dashed and dotted lines represent the experimental and calculated spectral data and the component deconvoluted B terms, respectively. All the bands used in this analysis with the exception of the main Q*00* band are B terms. The n → π^* bands near 605 nm and its associated vibronic progression are indicated. The residual of the fit plotted at the bottom of the plot shows the difference between the experimental and calculated MCD data. Reproduced with permission from ref 36. Copyright 1995 American Chemical Society.

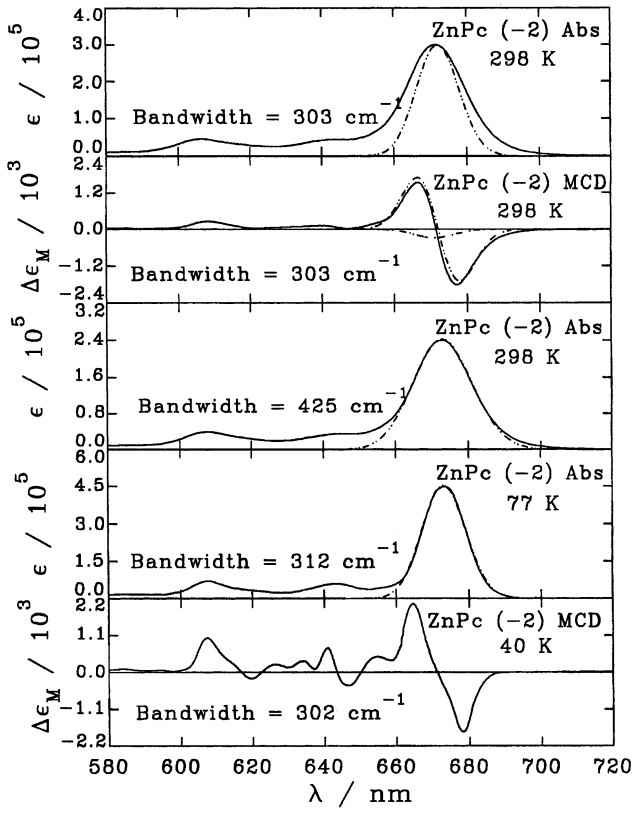

Figure 12. Temperature dependence in the Q band region of the UV−vis absorption and MCD spectra of ZnPc(−2) in liquid and vitrified solutions. The Gaussian curves illustrate the bandwidth discrepancy in the room temperature data. Reproduced with permission from ref 36. Copyright 1995 American Chemical Society.

spectrum dominated by A terms provides further evidence to support this assignment.[36,54]

(c) Band Deconvolution: The B1/B2 Spectral Region. Spectral deconvolution of absorption and MCD spectra has indicated previously that there are two separate A terms under Gouterman's B band in the spectrum of MPc(−2) complexes.[3a,e,31−33,36] ZINDO calculations indicate that this is due to mixing of the B transition with a one-electron transition involving the $1b_{1u}$ orbital.[54] A very weak A term sometimes observed slightly to the red of the B1 band has been assigned to a second $\pi \rightarrow \pi^*$ transition between the a_{1u} HOMO and a degenerate orbital located primarily on the fused benzene periphery of the ring system that is not present in the case of MP(−2).[54] The band deconvolution analyses of the B region of the absorption and MCD spectra of Zn3BoN, Zn3B1N, Zncis2B2N, Zntrans2B2N, and Zn1B3N are shown in Figures 13 and 14. The B1, B2, and to a lesser extent the second $\pi \rightarrow \pi^*$ one-electron transitions are predicted to contribute intensity to the most prominent bands observed between 26000 and 32000 cm^{-1} for all five complexes, Tables 1−3 and Tables S1−S3 (Supporting Information). The B1 bands remain the most intense UV−vis absorption bands because of the high degree of orbital overlap between the frontier orbitals associated with the cyclic polyene. This allowed $\Delta M_L = \pm 1$ transition of the inner cyclic polyene also dominates the MCD spectra because of the OAM associated with these orbitals, Figures 13 and 14 and S4−S6 (Supporting Information). Comparison with the calculated absorption spectra, Tables 1−3 and S1−S3 (Supporting Information), indicates that the B1 band tends to be ca. 5000 cm^{-1} to the red of the values predicted in the ZINDO calculations. The second $\pi \rightarrow \pi^*$ band shifts to the red as the orbitals corresponding to the $2e_g^*$ orbital of ZnPc(−2), which are associated primarily with the four peripheral benzo-groups, lie at higher energy relative to the HOMO orbital in most of the fused-ring substituted complexes, Table 4. The weaker bands to the blue of the B1 bands, Figures 13 and 14 and S4−S6 (Supporting Information), arise primarily from one-electron transitions involving both the inner cyclic polyene ring and the new peripheral fused rings. The original N/L/C band assignment terminology, which has previously been applied to the experimental spectra of MPc(−2),[54] is, therefore, clearly no longer directly applicable when there is an asymmetric extension to the π-system through the addition of peripheral fused rings.

Conclusions

Although the assignment of all the NMR signals for the asymmetric fused-ring-substituted complexes was relatively straightforward, some of the shifts observed for Zntrans2B2N and Zn3BoN do not correspond with the standard ring current

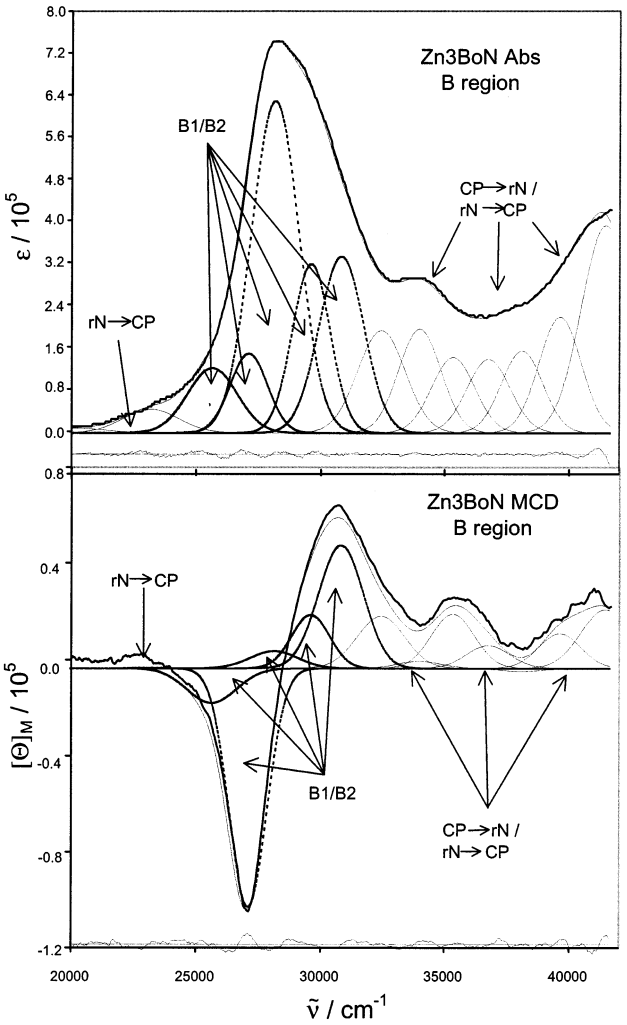

Figure 13. Spectral band deconvolution analysis of the B1/B2 spectral region of Zn3BoN. The band fitting parameters can be found in Table S9. Major electronic bands assigned in Table 2 to the B1 and B2 transitions, Figure 3, are shown in bold. The line showing the experimental MCD spectrum has been shifted positive slightly for visual purposes only.

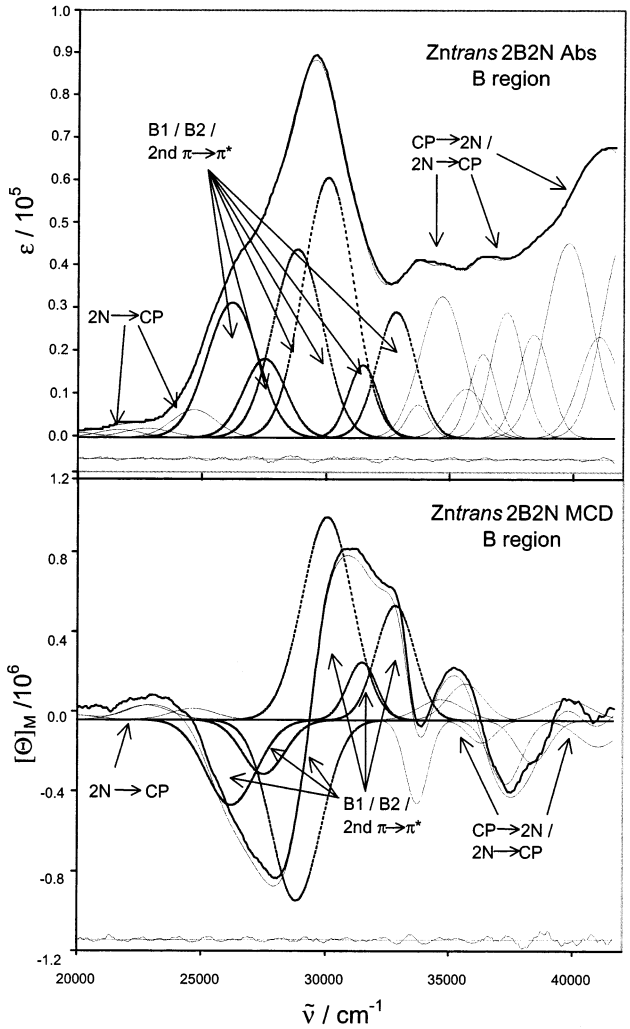

Figure 14. Spectral band deconvolution analysis of the B1/B2 spectral region of Zntrans2B2N. The band fitting parameters can be found in Table S12. Major electronic bands assigned in Table 3 to the B1 and B2 transitions, Figure 3, are shown in bold. The line showing the experimental MCD spectrum has been shifted positive slightly for visual purposes only.

interpretation developed previously to account for the NMR spectra of MP(−2) and MPc(−2) complexes. The optical spectra of Zntrans2B2N and Zn3BoN are also markedly different from those of Zn1B3N, Zncis2B2N, and Zn3B1N because there is a more marked symmetry-induced splitting in the Q spectral region. The bands associated primarily with the Q and B1 one-electron transitions of the 16-atom 18-π-electron inner cyclic polyene remain the dominant features in the spectra of all five complexes. The direct relevance of band assignment models developed previously for MPc(−2) complexes is, however, more limited in the UV region than was the case with partially aza-substituted complexes.[37] ZINDO/s calculations indicate the presence of additional MOs associated primarily with the additional peripheral fused benzene rings at energies similar to the $1a_{2u}$ orbital of MPc(−2). The spectral impact of these orbitals is most pronounced in the spectrum of Zn1B3N. The Φ_F values, NMR spectroscopy, and spectral band deconvolution analyses of the optical spectra identify Zntrans2B2N as the complex with the most substantially modified electronic properties relative to ZnPc(−2). Complexes based on this asymmetric fused ring pattern therefore probably have the most potential for use in new industrial applications.

Acknowledgment. J.M. and M.J.S. thank NSERC of Canada for Operating and Equipment grants (to M.J.S.) and support from Fujitsu Cache Inc. in providing software. M.J.S. is a member of the Centre for Chemical Physics at UWO.

Supporting Information Available: Calculated UV−vis spectra (Tables S1−S3), spectral band deconvolution analyses of the Q (Figures S1−S3) and B1/B2 (Figures S4−S6) spectral regions of Zn3B1N, Zncis2B2N, and Zn1B3N. Band fitting parameters from SIMPFIT deconvolution analyses of the Q and B1/B2 spectral regions (Tables S4−S13) of Zn3BoN, Zn3B1N, Zncis2B2N, Zntrans2B2N, and Zn1B3N. This material is available free of charge via the Internet at http://pubs.acs.org.

IC011152D